# Infinitesimally thin dielectric materials: Thickness dependencies in dielectric functions and Casimir energies*

Prachi Parashar† and Kimball A. Milton‡
*Oklahoma Center for High Energy Physics and Homer L. Dodge Department of Physics and Astronomy, University of Oklahoma, Norman, OK 73019, USA.*

M. Schaden§ and K. V. Shajesh¶
*Department of Physics, Rutgers, The State University of New Jersey, 101 Warren Street, Newark, NJ - 07102, USA.*

(Dated: October 19, 2011)

For pedagogy and as a learning exercise we present the details of the derivation for the Casimir energy between parallel dielectric slabs. We begin by deriving the multiple scattering formula for Casimir energy and use the Green's dyadic formalism. The general expression derived for the Casimir energy is independent of dielectric models and leads to standard results in limiting cases. The ideal conductor limit leads to the Casimir energy between two ideal conducting plates. The dilute dielectric limit gives the retarded van der Waals–London (Casimir-Polder) energy between weak dielectric slabs. Lifshitz formula is reproduced in the limit of thickness of each plate going to infinity. The Casimir energy between very thin dielectric plates is seemingly zero when standard dielectric models are used to model the plates. We duduce the dielectric function describing a slab to be

$$[\varepsilon(\omega) - 1]\omega^2 = -\frac{\lambda(\omega)}{d}$$

given in terms of a modified dielectric function $\lambda(\omega)$ assumed to be independent of thickness $d$ of the slab. Using the above model we are able to theoretically realize a $\delta$-function dielectric plate with its dielectric properties modeled by the modified dielectric function $\lambda(\omega)$.

Using the (modified) plasma model we calculate the Casimir energy between two $\delta$-function dielectric plates which is non-vanishing in contrast to the result obtained using standard dielectric models. In the ideal conductor limit this reproduces the standard Casimir energy. We also calculate the Casimir-Polder interaction energy between an atom and $\delta$-function dielectric slab, which again leads to the standard Casimir-Polder result in the ideal conductor limit.

We use our modified dielectric model to describe a graphene sheet. We calculate the Casimir interaction energy between two graphene sheets and a graphene sheet interacting with an ideal metal. We estimate the interlayer binding energy of graphite sheets and the exfoliation energy of graphene from graphite. We make the observation that weak approximation is sufficient to predict graphene-graphene interactions accurately.

---

* The contents of this paper has been extracted from Prachi Parashar's Ph.D. thesis.

†prachi@nhn.ou.edu
‡milton@nhn.ou.edu; http://www.nhn.ou.edu/~milton
§mschaden@andromeda.rutgers.edu; http://andromeda.rutgers.edu/~physics/mschaden.htm
¶shajesh@andromeda.rutgers.edu; http://andromeda.rutgers.edu/~shajesh

## CONTENTS



## I. VACUUM ENERGY

Electromagnetic fields consisting of the electric field $\mathbf{E}(\mathbf{x},t)$ and magnetic field $\mathbf{H}(\mathbf{x},t)$ interacting with macroscopic bodies described by the dielectric permittivity $\varepsilon(\mathbf{x},t)$ and magnetic permeability $\mu(\mathbf{x},t)$ of the material bodies involves the action in terms of the Lagrangian

$$W[\mathbf{E},\mathbf{H},\varepsilon,\mu] = \int d^3x \int dt\, \mathcal{L}(\mathbf{E},\mathbf{H},\varepsilon,\mu). \tag{1}$$

We will restrict ourselves to magnetic permeability $\mu = 1$. We shall neglect the dynamics (time dependence) of the dielectric bodies at the macroscopic level–for example we do not consider moving dielectrics. This still leaves us with two other venues for time dependence. First is the motion of electrons and nuclei forming the dielectric body at the microscopic level. This motion collectively contributes to the conductivity of a dielectric body, which will play a role in our study. The second form of time dependence is in the duration of the time for which a particular process is being investigated, which is introduced as the limits of integration of the time in Eq. (1). For most purposes it is sufficient to assume this time interval to be large enough to be replaced by $\pm\infty$. However, in the early nineteenth century while proposing a model for conductivity in metals Sommerfeld studied the signal velocity in a dispersive medium, and later Brillouin at Sommerfeld's suggestion in 1913, in a study of signal velocity in the wave propagation and its consequence on causality, noticed the necessity to keep track of this formal fallacy of infinite time interval [1]. In general this needs to be taken into account primarily in relation to questions related to causality and Nernt's heat theorem.

The electric susceptilbility defined as, (after suppressing the spatial dependence,)

$$\chi(t-t') = \varepsilon(t-t') - \delta(t-t') \tag{2}$$

codes the response of the system as induced polarization $\mathbf{P}(\mathbf{x},t)$ in the presence of an electric field

$$\mathbf{P}(t) = \int_{-\infty}^{\infty} dt'\, \varepsilon(t-t')\mathbf{E}(t'). \tag{3}$$

We have required translation invariance in time by imposing the dependence to be of the form $t-t'$. This effect should be causal and real which is suitably imposed by constructing

$$\chi(t-t') = \theta(t-t')f(t-t'), \qquad f^*(t) = f(t), \qquad f(-t) = -f(t), \tag{4}$$

where

$$\theta(t) = \begin{cases} 1 & \text{if} \quad t > 0, \\ 0 & \text{if} \quad t < 0. \end{cases} \tag{5}$$

The choice of $f(t)$ being an odd function is a convenient choice allowed due to the arbitraryness introduced by the $\theta$-function. The above statement of causality translates non-trivially into the frequency domain and is the content of Kramers-Kronig relations [2]. Using the Fourier transformations

$$f(t) = \int_{-\infty}^{\infty} \frac{d\omega}{2\pi}\, e^{-i\omega t}\tilde{f}(\omega) \tag{6}$$

and

$$\theta(t) = \lim_{\delta\to 0+} i\int_{-\infty}^{\infty} \frac{d\omega}{2\pi}\frac{e^{-i\omega t}}{\omega + i\delta}, \tag{7}$$

we can show that $\mathbf{P}(\omega) = \chi(\omega)\mathbf{E}(\omega)$, $\chi(\omega) = [\varepsilon(\omega) - 1]$, $\chi^*(\omega) = \chi(-\omega)$, $f^*(\omega) = f(-\omega)$, $\mathrm{Re}f(\omega) = 0$, and $\mathrm{Im}f(-\omega) = -\mathrm{Im}f(\omega)$. (We shall often drop the tilde on the functions.) We can then immediately derive (see [3]) the Kramers-Kronig relations

$$\mathrm{Im}\chi(\omega) = \frac{1}{2}\mathrm{Im}f(\omega), \tag{8}$$

$$\mathrm{Re}\chi(\omega) = \lim_{\delta\to 0+}\int_{-\infty}^{\infty} \frac{d\omega'}{2\pi}\frac{\omega'\mathrm{Im}f(\omega')}{[\omega'-\omega)^2 + \delta^2]}, \tag{9}$$

which implies that the real and imaginary parts of the dielectric susceptibility are manifestations of the same underlying property. The real part of susceptibility is square of refractive index of the material and relates to dispersion, and the imaginary part of dielectric susceptibilty relates to absorption. Kramers-Kronig relations explains the connection between anamolous dispersion and absorption observed in materials. Other optical properties like reflectance, transmission, and penetration depth are also given in terms of real and imaginary parts of susceptibility. Further, observing that a moving charge always looses energy to the medium, we can derive the positivity condition

$$\mathrm{Im}\chi(\omega) \geq 0, \quad \text{for} \quad \omega > 0, \tag{10}$$

and the sum-rule

$$\int_0^\infty d\omega\, \omega \mathrm{Im}\chi(\omega) = \frac{\pi}{2}\,\omega_p^2 \tag{11}$$

is deduced by requiring the high frequency behaviour to simulate a plasma. Here $\omega_p$ is a quantity depenendent on the charge density of the material, and is the plasma frequency for typical metals.

The Fourier transformed action after the introduction of the vector potential $\mathbf{A}(\mathbf{x},t)$ and scalar potential $\phi(\mathbf{x},t)$ is

$$W[\mathbf{E},\mathbf{H},\mathbf{A},\phi] = \int d^3x \int_{-\infty}^{\infty} \frac{d\omega}{2\pi}\,\mathcal{L}(\mathbf{E},\mathbf{H},\mathbf{A},\phi), \tag{12}$$

where the Fourier transformed Lagrangian density is

$$\begin{aligned}\mathcal{L}(\mathbf{E},\mathbf{H},\mathbf{A},\phi) = &-\frac{1}{2}\mathbf{E}(\mathbf{x},-\omega)\cdot\varepsilon(\mathbf{x},\omega)\mathbf{E}(\mathbf{x},\omega) + \mathbf{E}(\mathbf{x},-\omega)\cdot\varepsilon(\mathbf{x},\omega)\big[-\boldsymbol{\nabla}\phi(\mathbf{x},\omega) + i\omega\mathbf{A}(\mathbf{x},\omega))\big] \\ &+\frac{1}{2}\mathbf{H}(\mathbf{x},-\omega)\cdot\mathbf{H}(\mathbf{x},\omega) - \mathbf{H}(\mathbf{x},-\omega)\cdot[\boldsymbol{\nabla}\times\mathbf{A}(\mathbf{x},\omega)] + \mathbf{P}(\mathbf{x},-\omega)\cdot\big[-\boldsymbol{\nabla}\phi(\mathbf{x},\omega) + i\omega\mathbf{A}(\mathbf{x},\omega)\big].\end{aligned} \tag{13}$$

In general, the medium could be anisotropic and magnetic in which case the dielectric permittivity and permeability will be tensors. In this thesis we focus on non-magnetic, linear, isotropic, dispersive medium where $\mu(\mathbf{x},\omega) = 1$. Using the least action principle we obtain

$$\delta\mathbf{H}: \qquad \mathbf{H}(\mathbf{x},\omega) = \boldsymbol{\nabla}\times\mathbf{A}(\mathbf{x},\omega), \tag{14a}$$

$$\delta\mathbf{E}: \qquad \mathbf{E}(\mathbf{x},\omega) = -\boldsymbol{\nabla}\phi(\mathbf{x},\omega) + i\omega\mathbf{A}(\mathbf{x},\omega), \tag{14b}$$

$$\delta\mathbf{A}: \qquad \boldsymbol{\nabla}\times\mathbf{H}(\mathbf{x},\omega) = -i\omega\Big[\varepsilon(\mathbf{x},\omega)\mathbf{E}(\mathbf{x},\omega) + \mathbf{P}(\mathbf{x},\omega)\Big], \tag{14c}$$

$$\delta\phi: \qquad \boldsymbol{\nabla}\cdot\Big[\varepsilon(\mathbf{x},\omega)\mathbf{E}(\mathbf{x},\omega) + \mathbf{P}(\mathbf{x},\omega)\Big] = 0. \tag{14d}$$

The homogeneous Maxwell's equations can be obtained by taking the curl of the electric field and the divergence of the magnetic field, which we list here for completeness.

$$\boldsymbol{\nabla}\times\mathbf{E}(\mathbf{x},\omega) = i\omega\mathbf{H}(\mathbf{x},\omega), \tag{15a}$$

$$\boldsymbol{\nabla}\cdot\mathbf{H}(\mathbf{x},\omega) = 0,. \tag{15b}$$

The Maxwell's equations in Eqs. (14c) and (15a), in the frequency domain are

$$\boldsymbol{\nabla}\times\mathbf{E}(\mathbf{x},\omega) = i\omega\mathbf{H}(\mathbf{x},\omega), \tag{16a}$$

$$\boldsymbol{\nabla}\times\mathbf{H}(\mathbf{x},\omega) = -i\omega\Big[\varepsilon(\mathbf{x},\omega)\mathbf{E}(\mathbf{x},\omega) + \mathbf{P}(\mathbf{x},\omega)\Big]. \tag{16b}$$

Divergence of Eqs. (16a) and (16b) corresponds to Eqs. (15b) and (14d) in the frequency domain. Using Eq. (16a) in Eq. (16b) we have

$$-\big[\boldsymbol{\nabla}\times\boldsymbol{\nabla}\times\ -\omega^2\varepsilon(\mathbf{x},\omega)\mathbf{1}\big]\cdot\mathbf{E}(\mathbf{x},\omega) = -\omega^2\mathbf{P}(\mathbf{x},\omega). \tag{17}$$

Eq. (17) guides us to define the electric Green's dyadic satisfying the differential equation

$$-\left[-\frac{1}{\omega^2}\boldsymbol{\nabla}\times\boldsymbol{\nabla}\times\ +\varepsilon(\mathbf{x},\omega)\mathbf{1}\right]\cdot\boldsymbol{\Gamma}(\mathbf{x},\mathbf{x}';\omega) = \mathbf{1}\delta^{(3)}(\mathbf{x}-\mathbf{x}'), \tag{18}$$

and also defines the relation between the electric field and polarization source, mediated through the electric Green's dyadic $\boldsymbol{\Gamma}(\mathbf{x},\mathbf{x}';\omega)$,

$$\mathbf{E}(\mathbf{x},\omega) = \int d^3x'\,\boldsymbol{\Gamma}(\mathbf{x},\mathbf{x}';\omega)\cdot\mathbf{P}(\mathbf{x}',\omega). \tag{19}$$

The vacuum persistence amplitude is defined by

$$Z[\mathbf{P}] = \langle 0_+|0_-\rangle^{\mathbf{P}}. \tag{20}$$

We use Schwinger's quantum action principle [4–10]

$$\delta Z = i\langle 0_+|\delta W[\mathbf{E},\mathbf{H},\mathbf{A},\phi;\mathbf{P}]|0_-\rangle. \tag{21}$$

The variation with respect to the fields $\mathbf{E}$, $\mathbf{H}$, $\mathbf{A}$, and $\phi$ reproduces the equations of motion given in Eq. (14) when interpreted as equations for operator fields. Variation with respect to the external source $\mathbf{P}$ gives us

$$\delta\mathbf{P}: \qquad \delta Z = i\int d^3x \int_{-\infty}^{\infty} \frac{d\omega}{2\pi}\, \delta\mathbf{P}(\mathbf{x},-\omega)\, \langle 0_+|\mathbf{E}(\mathbf{x},\omega)|0_-\rangle^{\mathbf{P}}, \tag{22}$$

which implies

$$\frac{1}{i}\frac{\delta Z[\mathbf{P}]}{\delta\mathbf{P}(\mathbf{x},-\omega)} = \langle 0_+|\mathbf{E}(\mathbf{x},\omega)|0_-\rangle^{\mathbf{P}}. \tag{23}$$

Using this in Eq. (17) we can write

$$-\left[-\frac{1}{\omega^2}\boldsymbol{\nabla}\times\boldsymbol{\nabla}\times\ +\varepsilon(\mathbf{x},\omega)\mathbf{1}\right]\cdot\frac{1}{Z[\mathbf{P}]}\frac{1}{i}\frac{\delta Z[\mathbf{P}]}{\delta\mathbf{P}(\mathbf{x},-\omega)} = \mathbf{P}(\mathbf{x},\omega). \tag{24}$$

Notice that operator in square brackets is $\boldsymbol{\Gamma}^{-1}$ using Eq. (18). So, we can write the vacuum expectation value of $\mathbf{E}$ given by Eq. (24) using above equation as

$$\frac{1}{Z[\mathbf{P}]}\frac{1}{i}\frac{\delta Z[\mathbf{P}]}{\delta\mathbf{P}(\mathbf{x},-\omega)} = \int d^3x\, \boldsymbol{\Gamma}(\mathbf{x},\mathbf{x}';\omega)\cdot\mathbf{P}(\mathbf{x}',\omega)\,. \tag{25}$$

We can solve this functional differential equation for $Z[\mathbf{P}]$. One possible solution is

$$Z[\mathbf{P}] = Z[0]e^{\frac{i}{2}\int\frac{d\omega}{2\pi}\int d^3x\int d^3x'\mathbf{P}(\mathbf{x},-\omega)\cdot\boldsymbol{\Gamma}(\mathbf{x},\mathbf{x}';\omega)\cdot\mathbf{P}(\mathbf{x}',\omega)+Q[\varepsilon]}, \tag{26}$$

where $Q[\varepsilon]$ is a constant in $\mathbf{P}$. The argument of the exponential in above equation is defined as the effective action $W\big[\mathbf{P}\big]$. In absence of the background potential, i.e. for $\varepsilon = 1$, the effective action is given by

$$W_0[\mathbf{P}] = \frac{1}{2}\int_{-\infty}^{\infty}\frac{d\omega}{2\pi}\int d^3x\int d^3x'\,\mathbf{P}(\mathbf{x},-\omega)\cdot\boldsymbol{\Gamma}_0(\mathbf{x},\mathbf{x}';\omega)\cdot\mathbf{P}(\mathbf{x}',\omega)\ +\ Q[1], \tag{27}$$

where, $\boldsymbol{\Gamma}_0(\mathbf{x},\mathbf{x}';\omega)$ is the free Green's dyadic when no boundary is present and it satisfies

$$-\left[-\frac{1}{\omega^2}\boldsymbol{\nabla}\times\boldsymbol{\nabla}\times\ +\mathbf{1}\right]\cdot\boldsymbol{\Gamma}_0(\mathbf{x},\mathbf{x}';\omega) = \mathbf{1}\delta^{(3)}(\mathbf{x}-\mathbf{x}'). \tag{28}$$

Next if we switch off the external source as well then vacuum does not decay and can be written in terms of a constant phase $\theta$

$$Z_0[0] = \langle 0_+|0_-\rangle^{\mathbf{P}=0} = e^{i\theta} = e^{W_0[0]}. \tag{29}$$

This implies that $Q[1] = \theta$, which is a pure constant. Varying the vacuum persistence amplitude with respect to the background potential parameter $\varepsilon(\mathbf{x},\omega)$ we get

$$\begin{aligned}\delta\varepsilon(\mathbf{x},\omega): \qquad \delta Z[\mathbf{P}] &= \frac{i}{2}\int_{-\infty}^{\infty}\frac{d\omega}{2\pi}\int d^3x\,\delta\varepsilon(\mathbf{x},-\omega)\langle 0_+|\mathbf{E}(\mathbf{x},-\omega)\cdot\mathbf{E}(\mathbf{x},\omega)|0_-\rangle^{\mathbf{P}}\\ &= \frac{i}{2}\int_{-\infty}^{\infty}\frac{d\omega}{2\pi}\int d^3x\,\delta\varepsilon(\mathbf{x},-\omega)\frac{1}{i}\frac{\delta}{\delta\mathbf{P}(\mathbf{x},\omega)}\frac{1}{i}\frac{\delta}{\delta\mathbf{P}(\mathbf{x},-\omega)}Z[\mathbf{P}].\end{aligned} \tag{30}$$

We can formally write the solution for this as

$$Z[\mathbf{P}] = e^{\frac{i}{2}\int\frac{d\omega}{2\pi}\int d^3x[\varepsilon(\mathbf{x},-\omega)-1]\frac{1}{i}\frac{\delta}{\delta\mathbf{P}(\mathbf{x},\omega)}\frac{1}{i}\frac{\delta}{\delta\mathbf{P}(\mathbf{x},-\omega)}}\ Z_0[\mathbf{P}], \tag{31}$$

which using Eq. (27) can be written as

$$Z[\mathbf{P}] = e^{\frac{i}{2}\int\frac{d\omega}{2\pi}\int d^3x[\varepsilon(\mathbf{x},-\omega)-1]\frac{1}{i}\frac{\delta}{\delta\mathbf{P}(\mathbf{x},\omega)}\frac{1}{i}\frac{\delta}{\delta\mathbf{P}(\mathbf{x},-\omega)}}\ e^{\frac{i}{2}\int\frac{d\omega}{2\pi}\int d^3x\int d^3x'\mathbf{P}(\mathbf{x},-\omega)\cdot\boldsymbol{\Gamma}_0(\mathbf{x},\mathbf{x}',\omega)\cdot\mathbf{P}(\mathbf{x}',\omega)+Q[1]}. \tag{32}$$

Notice that we can safely drop the term $Q[1]$ as it will not contribute to the solution. Using the exponential identity

$$e^{\frac{1}{2}\nabla^{\mathrm{T}}\cdot\mathbf{A}\cdot\nabla}e^{\frac{1}{2}\mathbf{x}^{\mathrm{T}}\cdot\mathbf{B}\cdot\mathbf{x}+\mathbf{c}^{\mathrm{T}}\cdot\mathbf{x}+r} = e^{\frac{1}{2}\mathbf{x}^{\mathrm{T}}\cdot\mathbf{B}\cdot\mathbf{K}\cdot\mathbf{x}+\mathbf{c}^{\mathrm{T}}\cdot\mathbf{K}\cdot\mathbf{x}+\frac{1}{2}\mathbf{c}^{\mathrm{T}}\cdot\mathbf{K}\cdot\mathbf{A}\cdot\mathbf{c}+r+\frac{1}{2}\mathrm{Tr}\ln\mathbf{K}}, \tag{33}$$

for matrices where $\mathbf{K}$ is the solution to the matrix equation

$$\Big[\mathbf{1} - \mathbf{A}\cdot\mathbf{B}\Big]\cdot\mathbf{K} = \mathbf{1}, \tag{34}$$

we conclude that

$$Z[\mathbf{P}] = e^{\frac{i}{2}\int\frac{d\omega}{2\pi}\int d^3x\int d^3x'\mathbf{P}(\mathbf{x},-\omega)\cdot\mathbf{\Gamma}(\mathbf{x},\mathbf{x}';\omega)\cdot\mathbf{P}(\mathbf{x}',\omega) + 2\pi\delta(0)\frac{i}{2}\int\frac{d\omega}{2\pi}\,\mathrm{Tr}\ln\mathbf{\Gamma}\mathbf{\Gamma_0}^{-1}}, \tag{35}$$

where we have used Green's dyadic equation to obtain final form. The trace is over space variables only. Trace over the frequency domain leads to $2\pi\delta(0)$ which will be interpreted as the inifnite time $\tau$ of the process. For $Z[0]$ we get

$$Z[0] = \langle 0_+|0_-\rangle^{\mathbf{P}=0} = e^{iW[0]} = e^{\tau\frac{1}{2}\int\frac{d\omega}{2\pi}\,\mathrm{Tr}\ln\mathbf{\Gamma}\mathbf{\Gamma_0}^{-1}}. \tag{36}$$

Since $\langle 0_+|0_-\rangle^{\mathbf{P}=0} = \langle 0_-|e^{-iH\tau}|0_-\rangle^{\mathbf{P}=0} = e^{-iE\tau}$, comparing with above equation we conclude that

$$E - E_0 = \frac{i}{2}\int_{-\infty}^{\infty}\frac{d\omega}{2\pi}\mathrm{Tr}\ln\mathbf{\Gamma}\mathbf{\Gamma}_0^{-1}. \tag{37}$$

This is the principal formula we will use for calculating the Casimir energy. It is worth noting that the total vacuum energy is given by the trace-log of the electric Green's dyadic only. While in the frequency domain, we place confidence in the so-called Euclidean postulate [11, 12], and switch to imaginary frequencies after a Euclidean rotation using $\omega \to i\zeta$. Correspondingly the dielectric function will be: $\varepsilon(\mathbf{x},\omega) \to \varepsilon(\mathbf{x}, i\zeta)$. This leads to

$$E - E_0 = -\frac{1}{2}\int_{-\infty}^{\infty}\frac{d\zeta}{2\pi}\mathrm{Tr}\ln\mathbf{\Gamma}\mathbf{\Gamma}_0^{-1}. \tag{38}$$

### A. Multiple scattering formalism

The energy calculated using the formula given by Eq. (38) is divergent. These divergences arise due to the bulk contribution, self energy of the background potential, and curvature and corners of the boundaries. We require regularization and renormalization procedures to obtain a finite expression. However, in the presence of two non-overlapping boundaries it is possible to extract a finite energy for the interaction between two rigid boundaries using the multiple scattering (MS) formalism, which is all we need to define the Casimir force experienced by the boundaries. Multiple scattering techniques have been in use for a very long time (see introduction of [13] for a brief review of MS techniques). Notice that in Eq. (38) we have already subtracted the infinite bulk contribution given by

$$E_0 = -\frac{1}{2}\int_{-\infty}^{\infty}\frac{d\zeta}{2\pi}\mathrm{Tr}\ln\mathbf{\Gamma}_0. \tag{39}$$

The free Green's dyadic $\mathbf{\Gamma}_0(\mathbf{x},\mathbf{x}';i\zeta)$ satisfies Eq. (28). Comparing Eqs. (18) and (28), it is suggestive to define a potential

$$\mathbf{V}(\mathbf{x},i\zeta) = \mathbf{1}\big[\varepsilon(\mathbf{x},i\zeta) - 1\big] \tag{40}$$

to rewrite Eq. (18) in the form

$$-\left[\frac{1}{\zeta^2}\boldsymbol{\nabla}\times\boldsymbol{\nabla}\times\ +\mathbf{1} + \mathbf{V}(\mathbf{x},i\zeta)\right]\cdot\mathbf{\Gamma}(\mathbf{x},\mathbf{x}';i\zeta) = \mathbf{1}\delta^{(3)}(\mathbf{x}-\mathbf{x}'). \tag{41}$$

This allows us to write the solution (in symbolic notation) for the Green's dyadic in the presence of a medium in terms of the free Green's dyadic, defined in Eq. (28) in the form

$$\mathbf{\Gamma}\cdot\mathbf{\Gamma}_0^{-1} = \big[\mathbf{1} - \mathbf{\Gamma}_0\cdot\mathbf{V}\big]^{-1}. \tag{42}$$

For a system described by two disjoint boundaries, the potential is given by

$$\mathbf{V} = \mathbf{V}_1 + \mathbf{V}_2. \tag{43}$$

Using this in Eq. (42) we can write

$$\begin{aligned}\boldsymbol{\Gamma}\cdot\boldsymbol{\Gamma}_0^{-1} =&\boldsymbol{\Gamma}_2\cdot\boldsymbol{\Gamma}_0^{-1}\big[\mathbf{1}-\boldsymbol{\Gamma}_1\cdot\mathbf{V}_1\cdot\boldsymbol{\Gamma}_2\cdot\mathbf{V}_2\big]\boldsymbol{\Gamma}_1\cdot\boldsymbol{\Gamma}_0^{-1}\\ =&\big[\mathbf{1}-\boldsymbol{\Gamma}_0\cdot\mathbf{V}_2\big]^{-1}\big[\mathbf{1}-\boldsymbol{\Gamma}_1\cdot\mathbf{V}_1\cdot\boldsymbol{\Gamma}_2\cdot\mathbf{V}_2\big]\big[\mathbf{1}-\boldsymbol{\Gamma}_0\cdot\mathbf{V}_1\big]^{-1}.\end{aligned} \tag{44}$$

Substituting this in Eq. (38) we get

$$E = E_0 + E_1 + E_2 + E_{12}, \tag{45}$$

where the self energy contributions of the individual potentials $E_i$ are given by

$$E_i - E_0 = -\frac{1}{2}\int_{-\infty}^{\infty}\frac{d\zeta}{2\pi}\mathrm{Tr}\ln\big[\mathbf{1}-\boldsymbol{\Gamma}_0\cdot\mathbf{V}_i\big]^{-1}, \qquad i=1,2, \tag{46}$$

which in general are divergent. The remaining part of the energy is the interaction term $E_{12}$ between two disjoint boundaries and is given by

$$E_{12} = \frac{1}{2}\int_{-\infty}^{\infty}\frac{d\zeta}{2\pi}\mathrm{Tr}\ln\big[\mathbf{1}-\boldsymbol{\Gamma}_1\cdot\mathbf{V}_1\cdot\boldsymbol{\Gamma}_2\cdot\mathbf{V}_2\big]. \tag{47}$$

$V_i$ refers to the potential describing single boundary and $\boldsymbol{\Gamma}_i$ refers to the Green's dyadic when only one boundary is present. It is written in terms of the free Green's dyadic as

$$\boldsymbol{\Gamma}_i = \big[\mathbf{1}-\boldsymbol{\Gamma}_0\cdot\mathbf{V}_i\big]^{-1}\boldsymbol{\Gamma}_0. \tag{48}$$

We can define the $\mathbf{T}$-matrix as

$$\mathbf{T}_i = \mathbf{V}_i\big[\mathbf{1}-\boldsymbol{\Gamma}_0\cdot\mathbf{V}_i\big]^{-1}, \tag{49}$$

The interaction energy can be written in terms of $\mathbf{T}$-matrix as

$$E_{12} = \frac{1}{2}\int_{-\infty}^{\infty}\frac{d\zeta}{2\pi}\mathrm{Tr}\ln\big[\mathbf{1}-\boldsymbol{\Gamma}_0\cdot\mathbf{T}_1\cdot\boldsymbol{\Gamma}_0\cdot\mathbf{T}_2\big]. \tag{50}$$

The two expressions of the interaction energy given by Eq. (47) and Eq. (50) are equivalent. It is interesting to pause and think about the two forms. The Green's dyadic $\boldsymbol{\Gamma}_i$ describes the electromagnetic propagator in presence of the $i$-th boundary, which according to Eq. (48) is essentially the modification of the free propagator $\boldsymbol{\Gamma}_0$ due to the existing boundary. These modified propagators mediate between the two boundaries $\mathbf{V}_1$ and $\mathbf{V}_2$ causing interaction. On the other hand, the $\mathbf{T}_i$-matrix describes the modification of the potential $\mathbf{V}_i$ due to its own fluctuations. The information from one boundary is mediated to other boundary by free propagators causing interaction. The former approach is what describes the fluctuating fields interacting with static bodies viewpoint, while the later approach describes the interaction of the fluctuating bodies (molecules) viewpoint.

In this thesis we will be considering the two disjoint background potentials and use Eq. (47) form of the interaction energy for evaluation of the Casimir energy. This allows us to subtract off the divergent bulk contribution as well as the self energy contributions from the individual potential from the onset.

## II. GREEN'S DYADIC

In the previous section we obtained the central formula given by Eq. (38) for evaluating the vacuum energy, which requires us to solve for the corresponding Green's dyadic for a given system. The Green's dyadic, as the name suggests, is a second rank tensor quantity having nine scalar components, which are coupled. The formal Green's function technique can be found in standard mathematical texts, for example, Chapter 7 of Morse and Feshbach [14]. This thesis concentrates on parallel plate geometry for the electromagnetic case and cylindrical geometry for the scalar case. Therefore, in this Section we outline the procedure for obtaining Green's dyadic for the parallel geometry. We will present the scalar Green's function for the cylindrical case in the next chapter.

### A. Free Green's dyadic

We start with the free Green's dyadic $\mathbf{\Gamma}_0$ that satisfies Eq. (28). Taking the divergence of Eq. (28) we have

$$\boldsymbol{\nabla} \cdot \mathbf{\Gamma}_0(\mathbf{x}, \mathbf{x}'; i\zeta) = \boldsymbol{\nabla} \delta^{(3)}(\mathbf{x} - \mathbf{x}'). \tag{51}$$

Using this in conjunction with the identity

$$\boldsymbol{\nabla} \times (\boldsymbol{\nabla} \times \mathbf{\Gamma}_0) = (\boldsymbol{\nabla}\boldsymbol{\nabla} - \mathbf{1}\nabla^2) \cdot \mathbf{\Gamma}_0, \tag{52}$$

we can write Eq. (28) as

$$-[\nabla^2 - \zeta^2]\mathbf{\Gamma}_0(\mathbf{x}, \mathbf{x}'; i\zeta) = -\zeta^2 \mathbf{1} \delta^{(3)}(\mathbf{x} - \mathbf{x}') + \boldsymbol{\nabla}\boldsymbol{\nabla} \delta^{(3)}(\mathbf{x} - \mathbf{x}'). \tag{53}$$

In the frequency domain the scalar Green's function $G_0$ satisfies the equation

$$-[\nabla^2 - \zeta^2] G_0(\mathbf{x}, \mathbf{x}'; i\zeta) = \delta^{(3)}(\mathbf{x} - \mathbf{x}'). \tag{54}$$

The free Green's dyadic now has the formal solution in terms of free Green's scalar as

$$\mathbf{\Gamma}_0(\mathbf{x}, \mathbf{x}'; i\zeta) = [\boldsymbol{\nabla}\boldsymbol{\nabla} - \zeta^2 \mathbf{1}] G_0(\mathbf{x}, \mathbf{x}'; i\zeta). \tag{55}$$

We will write an explicit form for this in the next chapter.

### B. Green's dyadic equations

Next we turn our attention to the general Green's dyadic in in the presence of restrictive boundaries. For a non-magnetic, linear, isotropic, dispersive medium we wrote the differential equation satisfied by $\mathbf{\Gamma}$ in Eq. (41)

$$-\left[\frac{1}{\zeta^2}\boldsymbol{\nabla} \times \boldsymbol{\nabla} \times \; + \mathbf{1} + \mathbf{V}(\mathbf{x}, i\zeta)\right] \cdot \mathbf{\Gamma}(\mathbf{x}, \mathbf{x}'; i\zeta) = \mathbf{1} \delta^{(3)}(\mathbf{x} - \mathbf{x}'), \tag{56}$$

which is related to the electric field and the polarization source as

$$\mathbf{E}(\mathbf{x}, i\zeta) = \int d^3x' \, \mathbf{\Gamma}(\mathbf{x}, \mathbf{x}'; i\zeta) \cdot \mathbf{P}(\mathbf{x}', i\zeta). \tag{57}$$

Eq. (56) is a second order differential equation coupling the scalar components of the Green's dyadic. Using the free Green's dyadic Eq. (28) we can formally write the solution for the Green's dyadic as given in Eq. (48)

$$\mathbf{\Gamma} = \big[\mathbf{1} - \mathbf{\Gamma}_0 \cdot \mathbf{V}\big]^{-1} \mathbf{\Gamma}_0. \tag{58}$$

This can be written as an infinite series and getting an explicit solution for the Green's dyadic depends on the potential describing the boundary and in turn on the boundary conditions imposed by it. As it turns out, it is not a trivial task. Even for the simple case of a step function potential re-summing the series is very difficult. In order to proceed further and keeping our goal of solving for the parallel geometry in mind we use techniques in [15] and define the corresponding magnetic Green's function $\mathbf{\Phi}(\mathbf{x}, \mathbf{x}'; i\zeta)$

$$\mathbf{H}(\mathbf{x}, i\zeta) = \int d^3x' \, \mathbf{\Phi}(\mathbf{x}, \mathbf{x}'; i\zeta) \cdot \mathbf{P}(\mathbf{x}', i\zeta). \tag{59}$$

In terms of the electric and magnetic Green's dyadic, defined in Eqs. (57) and (59), the Maxwell's equations given by Eqs. (16) are contained in

$$-\boldsymbol{\nabla} \times \mathbf{\Gamma}(\mathbf{x}, \mathbf{x}'; i\zeta) = \zeta \mathbf{\Phi}(\mathbf{x}, \mathbf{x}'; i\zeta), \tag{60a}$$

$$\boldsymbol{\nabla} \times \mathbf{\Phi}(\mathbf{x}, \mathbf{x}'; i\zeta) = \zeta \big[\varepsilon(\mathbf{x}, i\zeta) \mathbf{\Gamma}(\mathbf{x}, \mathbf{x}'; i\zeta) + \mathbf{1} \delta^{(3)}(\mathbf{x} - \mathbf{x}')\big]. \tag{60b}$$

This is illustrated by taking the dot-product of Eqs. (60) with $\mathbf{P}$ on the right and taking the integral over $x'$, which reproduces the expressions in Eqs. (16). The homogenous equations given by Eq. (15) can be obtained, similarly, by taking divergence from the left. Using Eq. (60a) in Eq. (60b) gives the second order differential equation for the Green's dyadic given in Eq. (18). The above equations are coupled first order differential equations. This doesn't reduce the amount of work; however, it provides a framework for solving the Green's dyadic for the case of a step potential (parallel geometry) as we shall see in next section.

### C. Planar geometries

Consider the physical situations involving translational symmetry in the $x$-$y$ directions. We begin by writing the Green's dyadic and the unit operator in terms of basis vectors

$$\mathbf{\Gamma} = \mathbf{\Gamma}_x\hat{\mathbf{x}} + \mathbf{\Gamma}_y\hat{\mathbf{y}} + \mathbf{\Gamma}_z\hat{\mathbf{z}}, \tag{61a}$$

$$\mathbf{\Phi} = \mathbf{\Phi}_x\hat{\mathbf{x}} + \mathbf{\Phi}_y\hat{\mathbf{y}} + \mathbf{\Phi}_z\hat{\mathbf{z}}, \tag{61b}$$

$$\mathbf{1} = \hat{\mathbf{x}}\,\hat{\mathbf{x}} + \hat{\mathbf{y}}\,\hat{\mathbf{y}} + \hat{\mathbf{z}}\,\hat{\mathbf{z}}. \tag{61c}$$

In this case the potential given by Eq. (40) depends on the $z$-coordinate

$$V(z) = [\varepsilon(z) - 1]. \tag{62}$$

Using a Fourier transform in $x$-$y$ directions we can define the dimensionally reduced dyadic

$$\mathbf{\Gamma}(\mathbf{x}, \mathbf{x}'; i\zeta) = \int \frac{d^2k}{(2\pi)^2}\, e^{i\mathbf{k}_\perp\cdot(\mathbf{x}-\mathbf{x}')_\perp}\boldsymbol{\gamma}(z, z'; i\zeta, k), \tag{63a}$$

$$\mathbf{\Phi}(\mathbf{x}, \mathbf{x}'; i\zeta) = \int \frac{d^2k}{(2\pi)^2}\, e^{i\mathbf{k}_\perp\cdot(\mathbf{x}-\mathbf{x}')_\perp}\boldsymbol{\phi}(z, z'; i\zeta, k), \tag{63b}$$

where $\mathbf{k}_\perp^2 = k_x^2 + k_y^2 = k^2$. Due to rotational symmetry in the $x$-$y$ directions we can choose $k_y = 0, k_x = k$, without any loss of generality. Using Eqs. (61) and (63) in Eq. (60) we have

$$\boldsymbol{\phi}_x = \frac{1}{\zeta}\frac{\partial}{\partial z}\boldsymbol{\gamma}_y, \tag{64a}$$

$$\boldsymbol{\phi}_y = -\frac{1}{\zeta}\frac{\partial}{\partial z}\boldsymbol{\gamma}_x + i\frac{k}{\zeta}\boldsymbol{\gamma}_z, \tag{64b}$$

$$\boldsymbol{\phi}_z = -i\frac{k}{\zeta}\boldsymbol{\gamma}_y. \tag{64c}$$

and

$$\boldsymbol{\gamma}_x = \frac{1}{\zeta}\frac{1}{\varepsilon(z)}\frac{\partial}{\partial z}\boldsymbol{\phi}_y - \frac{\delta(z-z')}{\varepsilon(z)}\hat{\mathbf{x}}, \tag{65a}$$

$$\boldsymbol{\gamma}_y = \frac{1}{\zeta}\frac{1}{\varepsilon(z)}\frac{\partial}{\partial z}\boldsymbol{\phi}_x - i\frac{k}{\zeta}\frac{1}{\varepsilon(z)}\boldsymbol{\phi}_z - \frac{\delta(z-z')}{\varepsilon(z)}\hat{\mathbf{y}}, \tag{65b}$$

$$\boldsymbol{\gamma}_z = i\frac{k}{\zeta}\frac{1}{\varepsilon(z)}\boldsymbol{\phi}_y - \frac{\delta(z-z')}{\varepsilon(z)}\hat{\mathbf{z}}. \tag{65c}$$

Using Eqs. (64a) and (64c) in Eq. (65b) we obtain the differential equation for $\gamma_y$ to be

$$-\left[\frac{\partial^2}{\partial z^2} - k^2 - \zeta^2\varepsilon(z)\right]\boldsymbol{\gamma}_y(z, z'; i\zeta, k) = -\zeta^2\,\hat{\mathbf{y}}\,\delta(z-z'). \tag{66}$$

Similarly using Eqs. (65a) and (65c) in Eq. (64b) we have

$$-\left[\frac{\partial}{\partial z}\frac{1}{\varepsilon(z)}\frac{\partial}{\partial z} - \frac{k^2}{\varepsilon(z)} - \zeta^2\right]\boldsymbol{\phi}_y(z, z'; i\zeta, k) = -i\hat{\mathbf{z}}\,\frac{k\zeta}{\varepsilon(z)}\delta(z-z') + \hat{\mathbf{x}}\,\frac{\zeta}{\varepsilon(z)}\frac{\partial}{\partial z}\delta(z-z'). \tag{67}$$

Let us now define reduced electric $g^E(z, z')$ and magnetic $g^H(z, z')$ scalar Green's functions[1] which satisfy

$$-\left[\frac{\partial^2}{\partial z^2} - k^2 - \zeta^2\varepsilon(z)\right]g^E(z, z') = \delta(z-z'), \tag{68a}$$

$$-\left[\frac{\partial}{\partial z}\frac{1}{\varepsilon(z)}\frac{\partial}{\partial z} - \frac{k^2}{\varepsilon(z)} - \zeta^2\right]g^H(z, z') = \delta(z-z'). \tag{68b}$$

---

[1] Here we use the notation in Schwinger et al[15] which was reversed in many of Milton's publications, for example in Milton's book[16] and [17].

It is now straightforward to obtain $\boldsymbol{\gamma}_y$ and $\boldsymbol{\phi}_y$ in terms of $g^E$ and $g^H$ as

$$\boldsymbol{\gamma}_y(z,z';i\zeta,k) = -\hat{\mathbf{y}}\zeta^2 g^E(z,z'), \tag{69a}$$

$$\boldsymbol{\phi}_y(z,z';i\zeta,k) = -i\hat{\mathbf{z}}\,\frac{k\zeta}{\varepsilon(z')}g^H(z,z') - \hat{\mathbf{x}}\,\frac{\zeta}{\varepsilon(z')}\frac{\partial}{\partial z'}g^H(z,z'), \tag{69b}$$

where we integrated by parts to obtain the second term in the $\phi_y$ expression. The remaining components are completely given in terms of $\boldsymbol{\gamma}_y$ and $\boldsymbol{\phi}_y$ as

$$\boldsymbol{\phi}_x = \frac{1}{\zeta}\frac{\partial}{\partial z}\boldsymbol{\gamma}_y, \tag{70}$$

$$\boldsymbol{\phi}_z = -i\frac{k}{\zeta}\boldsymbol{\gamma}_y, \tag{71}$$

and

$$\boldsymbol{\gamma}_x = -\frac{1}{\zeta}\frac{1}{\varepsilon(z)}\frac{\partial}{\partial z}\boldsymbol{\phi}_y - \hat{\mathbf{x}}\frac{\delta(z-z')}{\varepsilon(z)}, \tag{72}$$

$$\boldsymbol{\gamma}_z = i\frac{k}{\zeta}\frac{1}{\varepsilon(z)}\boldsymbol{\phi}_y - \hat{\mathbf{z}}\frac{\delta(z-z')}{\varepsilon(z)}. \tag{73}$$

Using the above the electric and magnetic Green's dyadic are given in terms of the reduced Green's function as

$$\boldsymbol{\phi}(z,z';i\zeta,k) = \begin{bmatrix} 0 & -\zeta\frac{\partial}{\partial z}g^E(z,z') & 0 \\ -\frac{\zeta}{\varepsilon(z')}\frac{\partial}{\partial z'}g^H(z,z') & 0 & -\frac{ik\zeta}{\varepsilon(z')}g^H(z,z') \\ 0 & ik\zeta g^E(z,z') & 0 \end{bmatrix} \tag{74}$$

and

$$\boldsymbol{\gamma}(z,z';i\zeta,k) = \begin{bmatrix} \frac{1}{\varepsilon(z)}\frac{\partial}{\partial z}\frac{1}{\varepsilon(z')}\frac{\partial}{\partial z'}g^H(z,z') & 0 & \frac{ik}{\varepsilon(z)}\frac{1}{\varepsilon(z')}\frac{\partial}{\partial z}g^H(z,z') \\ 0 & -\zeta^2 g^E(z,z') & 0 \\ -\frac{ik}{\varepsilon(z)}\frac{1}{\varepsilon(z')}\frac{\partial}{\partial z'}g^H(z,z') & 0 & \frac{k^2}{\varepsilon(z)\varepsilon(z')}g^H(z,z') \end{bmatrix} - \frac{\delta(z-z')}{\varepsilon(z)}\begin{bmatrix} 1 & 0 & 0 \\ 0 & 0 & 0 \\ 0 & 0 & 1 \end{bmatrix}. \tag{75}$$

Thus for the physical situations involving translational symmetry in $x$ and $y$ directions and non-magnetic, linear, isotropic, dispersive medium the whole problem decouples to solving for two scalar transverse electric and transverse magnetic Green's function, which are subject to the boundary conditions imposed by the physical problem.

## III. GREEN'S FUNCTIONS

In the previous Section II, we presented the formal solution for the free Green's dyadic and the Green's dyadic in presence of a translationally symmetric background potential in terms of two free scalar Green's function. In this chapter we collect solutions to these scalar Green's function for the configurations we will be dealing in this thesis.

### A. Free scalar Green's function

In absence of any boundary the free Green's function $G_0(\mathbf{x},\mathbf{x}';i\zeta)$, which satisfies Eq. (54) has translational symmetry in all coordinates. Therefore it can depend only on $(\mathbf{x}-\mathbf{x}')$. In three dimensions the explicit solution is given by

$$G_0(\mathbf{x}-\mathbf{x}';i\zeta) = \frac{e^{-|\zeta||\mathbf{x}-\mathbf{x}'|}}{4\pi|\mathbf{x}-\mathbf{x}'|}. \tag{76}$$

If we assume translational invariance in $x$-dimension then we can Fourier transform one coordinate and write

$$G_0(\mathbf{x}-\mathbf{x}';i\zeta) = \int_{-\infty}^{\infty}\frac{dk_x}{2\pi}e^{ik_x(x-x')}g_0(\mathbf{x}_\perp-\mathbf{x}'_\perp;\kappa), \tag{77}$$

where $\kappa$ is defined by $\kappa^2 = \zeta^2 + k_x^2$. Then the two dimensional reduced Green's function $g_0(\mathbf{x}_\perp - \mathbf{x}'_\perp; \kappa)$ is written in terms of the modified Bessel function $K_0$ as

$$g_0(\mathbf{x}_\perp - \mathbf{x}'_\perp; \kappa) = \frac{1}{2\pi} K_0(\kappa |\mathbf{x}_\perp - \mathbf{x}'_\perp|). \tag{78}$$

If we assume assume translation symmetry in $x$–and $y$-directions and write

$$G_0(\mathbf{x} - \mathbf{x}'; i\zeta) = \int_{-\infty}^{\infty} \frac{dk_x}{2\pi} \int_{-\infty}^{\infty} \frac{dk_y}{2\pi}\, e^{i\mathbf{k}_\perp \cdot (\mathbf{x}-\mathbf{x}')_\perp} g_0(z - z'; \kappa), \tag{79}$$

where now $\kappa^2 = \zeta^2 + k_\perp^2$ with $k_\perp^2 = k_x^2 + k_y^2$. The one dimensional reduced Green's function $g_0(z - z'; \kappa)$ has the solution

$$g_0(z - z'; \kappa) = \frac{1}{2\kappa}\, \mathrm{e}^{-\kappa |z - z'|}. \tag{80}$$

### B. Green's function for a single $\delta$-function potential

For the sake of completeness we list the solution for the Green's function for a single semi-transparent $\delta$-function potential, described by $V = \lambda \delta(z - a)$, which satisfies

$$-\Big[\frac{\partial^2}{\partial z^2} - \kappa^2 - \lambda \delta(z - a)\Big] g(z, z'; \kappa) = \delta(z - z') \tag{81}$$

and has the solution

$$g(z, z'; \kappa) = \frac{1}{2\kappa}\, e^{-\kappa |z - z'|} - \frac{1}{2\kappa} \frac{\lambda}{\lambda + 2\kappa}\, e^{-\kappa |z-a|} e^{-\kappa |z' - a|}. \tag{82}$$

### C. Transverse electric Green's function

Next we turn our attention to the solution of the transverse electric Green's function for the case of translational symmetry in $x$-$y$ direction. The potential $\mathbf{V}(\mathbf{x}, i\zeta)$, described in Eq. (40), now has dependence on the $z$-coordinate only

$$V(z) = [\varepsilon(z) - 1]. \tag{83}$$

The differential equation for the electric Green's function in Eq. (68a) can be written as

$$-\left[\frac{\partial^2}{\partial z^2} - \kappa^2 - \zeta^2 V(z)\right] g^E(z, z'; \kappa) = \delta(z - z'), \tag{84}$$

where $\kappa^2 = \zeta^2 + k_\perp^2$.

#### 1. *Two layered dielectric medium*

Consider two dielectric media of permittivity $\varepsilon_1$ and $\varepsilon_2$ separated by a plane surface located at $z = a$ shown in Figure 1. This physical situation can be described by

$$V(z) = (\varepsilon_1 - 1)\theta(a - z) + (\varepsilon_2 - 1)\theta(z - a), \tag{85}$$

where $\theta(z - a) = 0$ if $z < a$, and $\theta(z - a) = 1$ if $z > a$. Using the matching conditions, which are (a) $g^E$ is continuous and (b) $\frac{d}{d\,z}\, g^E(z, z')$ is discontinuous across the boundary, we can solve the differential equation (68a). The solution for the electric Green's function is

$$g^E(z, z') = \frac{s_n}{\kappa_z + \kappa_{z'}}\, e^{-\kappa_z |z - z'|} + \frac{t_n}{\kappa_z + \kappa_{z'}}\, e^{-\kappa_z |z - a_i|} e^{-\kappa_{z'} |z' - a_i|}, \tag{86}$$

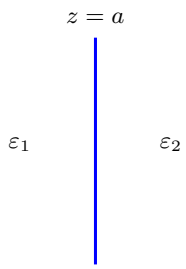


FIG. 1. Two layered dielectric material.

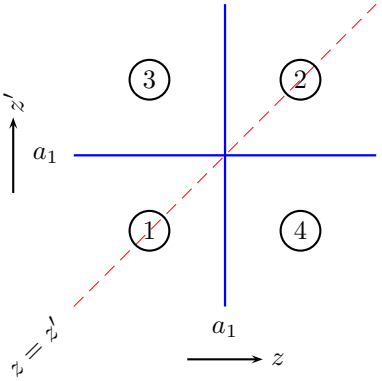


FIG. 2. Regions for investigation of the Green's function for the step potential.

where $n$ represents regions 1 to 4 in Figure 2. Coefficients $s_n = 1$ if $n = 1, 2$, and zero otherwise. This basically represents the bulk term and is present only when $z$ and $z'$ are in the same region. In the above equations $\kappa_z$ and $\kappa_{z'}$ take on values of $\kappa_i$ based on the regions in which the respective $z, z'$ are in. $\kappa_i^2 = k^2 + \zeta^2\varepsilon_i = \kappa^2 + \zeta^2(\varepsilon_i - 1)$ for $i = 1, 2$, and coefficients $t_n$ are given in Table I, where

$$\alpha_{ij} = \frac{\kappa_i - \kappa_j}{\kappa_i + \kappa_j}. \tag{87}$$

When one medium is vacuum, i.e. $\varepsilon \to 1$ for that medium, $\kappa' \to \kappa$ for that medium.

| | |
|---|---|
| $t_3 = 1$ | $t_2 = -\alpha_{ji}$ |
| $t_1 = \alpha_{ij}$ | $t_4 = 1$ |

TABLE I. Transition matrix coefficients for the two layered dielectric media.

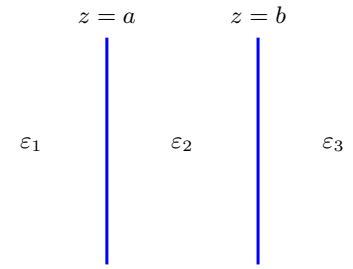


FIG. 3. Three layered dielectric material.

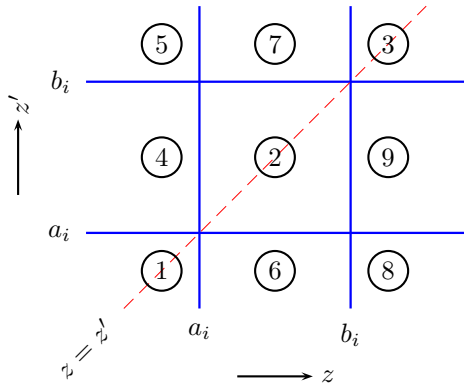


FIG. 4. Regions for investigation of the Green's function for the slab potential.

### 2. *Three layered dielectric medium–slab*

Next we consider three dielectric media separated by plane surfaces located at $z = a$ and $z = b$ as shown in Figure. 3, which can be described by the potential

$$V(z) = (\varepsilon_1 - 1)\theta(a - z) + (\varepsilon_2 - 1)\left[\theta(z - a) - \theta(b - z)\right] + (\varepsilon_3 - 1)\theta(z - b). \tag{88}$$

The middle slab has thickness $d = b - a$. The solution can be expressed in the form

$$g^E(z, z') = \frac{s_n}{\kappa_z + \kappa_{z'}}\, e^{-\kappa_z|z-z'|} + \mathbf{e}(z)^T \cdot \frac{1}{\Delta}\, \frac{\mathbf{t}_n}{\kappa_z + \kappa_{z'}} \cdot \mathbf{e}(z') \tag{89}$$

where $n$ denotes regions from 1 to 9 in Figure 4. The coefficients $s_n = 1$, if $n = 1, 2, 3$, and zero otherwise. The vector $\mathbf{e}(z)$ is defined in terms of the free Green's function as

$$\mathbf{e}(z)^T = \left( e^{-\kappa_z|z-a_i|},\ \ e^{-\kappa_z|z-b_i|} \right). \tag{90}$$

The determinant $\Delta$ is given by

$$\Delta = (1 - \alpha_{21}\alpha_{23}e^{-2\kappa_2 d}), \tag{91}$$

where $\kappa_2^2 = \kappa^2 + \zeta^2(\varepsilon_2 - 1)$. The coefficients $\mathbf{t}_n$s are given in Table III C 2. For the specific case when $\varepsilon_{1,3} = 1$ describes a dielectric slab. The solution can be obtained by setting $\kappa_{1,3} = \kappa$ in above equations. Subscript 2 used to identify the middle dielectric layer can be replaced by $i$ to denote $i$-th slab.

| | | |
|---|---|---|
| $\mathbf{t}_5 = \begin{bmatrix} 0 & (1-\alpha_{21}\alpha_{23})e^{-\kappa_2 d} \\ 0 & 0 \end{bmatrix}$ | $\mathbf{t}_7 = \begin{bmatrix} 0 & \alpha_{21}e^{-\kappa_2 d} \\ 0 & 1 \end{bmatrix}$ | $\mathbf{t}_3 = \begin{bmatrix} 0 & 0 \\ 0 & -(\alpha_{23}-\alpha_{21}e^{-2\kappa_2 d}) \end{bmatrix}$ |
| $\mathbf{t}_4 = \begin{bmatrix} 1 & \alpha_{23}e^{-\kappa_2 d} \\ 0 & 0 \end{bmatrix}$ | $\mathbf{t}_2 = \begin{bmatrix} \alpha_{21} & \alpha_{21}\alpha_{23}e^{-\kappa_2 d} \\ \alpha_{21}\alpha_{23}e^{-\kappa_2 d} & \alpha_{23} \end{bmatrix}$ | $\mathbf{t}_9 = \begin{bmatrix} 0 & 0 \\ \alpha_{21}e^{-\kappa_i d_i} & 1 \end{bmatrix}$ |
| $\mathbf{t}_1 = \begin{bmatrix} -(\alpha_{21}-\alpha_{23}e^{-2\kappa_2 d}) & 0 \\ 0 & 0 \end{bmatrix}$ | $\mathbf{t}_6 = \begin{bmatrix} 1 & 0 \\ \alpha_{23}e^{-\kappa_i d_i} & 0 \end{bmatrix}$ | $\mathbf{t}_8 = \begin{bmatrix} 0 & 0 \\ (1-\alpha_{21}\alpha_{23})e^{-\kappa_2 d} & 0 \end{bmatrix}$ |

TABLE II. Transition matrix coefficients for the three layered dielectric medium.

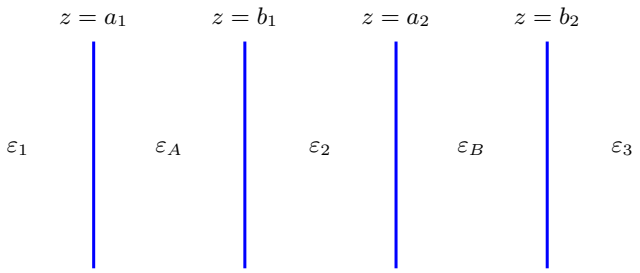


FIG. 5. Five layered dielectric material.

### 3. *Five layered dielectric medium*

Let us now consider the potential

$$\begin{aligned} V(z) = \quad & (\varepsilon_1 - 1)\theta(a_1 - z) + (\varepsilon_A - 1)\left[\theta(z - a_1) - \theta(z - b_1)\right] \\ & + (\varepsilon_2 - 1)\left[\theta(z - b_1) - \theta(z - a_2)\right] + (\varepsilon_B - 1)\left[\theta(z - a_2) - \theta(z - b_2)\right] \\ & + (\varepsilon_3 - 1)\theta(z - b_2), \end{aligned} \tag{92}$$

where $d_{1,2} = b_{1,2} - a_{1,2}$ and $a = a_2 - b_1$. The choice of subscript is governed by the fact that when $d_{1,2} \to 0$ we get potential described in the previous subsection. This is shown in Figure 5.
The solution can be written as before

$$g^E(z, z') = \frac{s_n}{\kappa_z + \kappa_{z'}} e^{-\kappa_z |z - z'|} + \mathbf{e}(z)^T \cdot \frac{1}{\Delta} \frac{\mathbf{t}_n}{\kappa_z + \kappa_{z'}} \cdot \mathbf{e}(z') \tag{93}$$

where $n$ denotes regions given in Figure 6. The coefficients $s_n = 1$, if $n = 1, 2, 3, A, B$, and zero otherwise. The vector $\mathbf{e}(z)$ is defined in terms of the free Green's function as

$$\mathbf{e}(z)^T = \left( e^{-\kappa_z |z - a_1|}, \;\; e^{-\kappa_z |z - b_1|}, e^{-\kappa_z |z - a_2|}, \;\; e^{-\kappa_z |z - b_2|} \right). \tag{94}$$

To save space we define

$$\delta_{11} = \alpha_{2A} + \alpha_{A1} e^{-2\kappa_A d_1} \tag{95a}$$
$$\delta_{12} = 1 + \alpha_{2A}\alpha_{A1} e^{-2\kappa_A d_1} \tag{95b}$$
$$\delta_{21} = 1 + \alpha_{2B}\alpha_{B3} e^{-2\kappa_B d_2} \tag{95c}$$
$$\delta_{22} = \alpha_{2B} + \alpha_{B3} e^{-2\kappa_B d_2} \tag{95d}$$

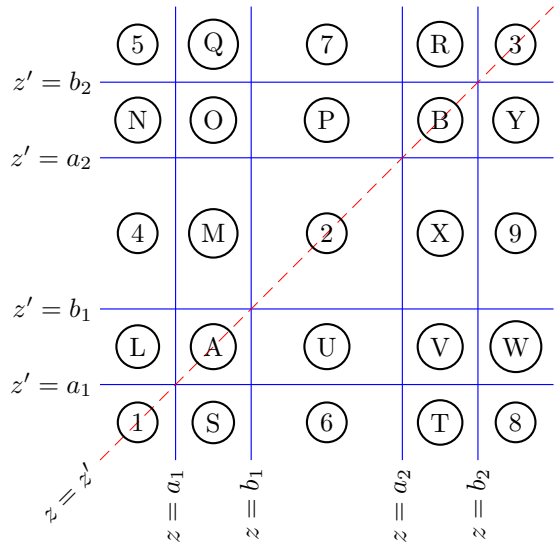


FIG. 6. Regions for investigation of five region Green's function.

Using these notations the determinant $\Delta$ is given by

$$\Delta = \delta_{11}\delta_{22}e^{-\kappa_2 a} - \delta_{12}\delta_{21}e^{\kappa_2 a}. \tag{96}$$

In Tables III and IV we give the non-vanishing components of the coefficients $\mathbf{t}_n$.

### D. Transverse magnetic Green's function

Solving for the transverse magnetic Green's function requires imposing physical boundary conditions on the Green's function solutions since its not possible to get both matching conditions on the boundary using Eq. (68b). Therefore, one condition needs to be fixed using the physical boundary conditions. For the electromagnetic field we know that $[\varepsilon\mathbf{E}]_3(z)$ is continuous on the boundary. Then using

$$\gamma_{33}(z,z') = \frac{1}{i}\langle \mathbf{E}_3(z)\mathbf{E}_3(z')\rangle, \tag{97}$$

and Eq. (75) and the continuity of $[\varepsilon\mathbf{E}]_3(z)$ we can conclude that $g^H(z,z')$ is continuous at the boundary of the two dielectric surfaces. This allows us to get the second condition from the Green's functions equation, which is

$$\left[-\frac{1}{\varepsilon(z)}\frac{\partial}{\partial z}g^H(z,z')\right]_{z=a-\epsilon}^{z=a+\epsilon} = 0. \tag{98}$$

The solution for the scalar magnetic Green's function for the two layered dielectric medium is

$$g^E(z,z') = \frac{s_n}{\overline{\kappa}_z + \overline{\kappa}_{z'}}\, e^{-\kappa_z|z-z'|} + \frac{t_n}{\overline{\kappa}_z + \overline{\kappa}_{z'}}\, e^{-\kappa_z|z-a_i|}e^{-\kappa_{z'}|z'-a_i|}, \tag{99}$$

where

$$\overline{\kappa}_z = \frac{\kappa_z}{\varepsilon(z)}. \tag{100}$$

This solution is similar to the scalar electric Green's function solution except that $\kappa_z$'s are replaced by $\overline{\kappa}_z$'s everywhere except in exponentials. This feature is generic for the $\theta$-potential, so we will use solutions of the electric Green's function for other cases described in the previous section and let $\kappa_i \to \overline{\kappa}_i$ everywhere except in the exponential.

| | | |
|---|---|---|
| $\mathbf{t}_5^{a_1b_2}=\big[(\alpha_{A1}+\alpha_{2A})(\alpha_{2B}+\alpha_{B3})$ $-(1+\alpha_{2A}\alpha_{A1})(1+\alpha_{2B}\alpha_{B3})\big]e^{-\kappa_A d_1-\kappa_B d_2}$ | $\mathbf{t}_Q^{b_1b_2}=-\big[\,(1-\alpha_{2A}\alpha_{2B})+\alpha_{B3}\,(\alpha_{2B}-\alpha_{2A})\,\big]e^{-\kappa_B d_2}$ $\mathbf{t}_Q^{a_1b_2}=\mathbf{t}_Q^{b_1b_2}\alpha_{A1}e^{-\kappa_A d_1}$ | $\mathbf{t}_7^{b_1b_2}=-\,(1+\alpha_{2B}\alpha_{B3})\,\delta_{11}e^{-\kappa_B d_2}$ $\mathbf{t}_7^{a_2b_2}=-\,(1+\alpha_{2B}\alpha_{B3})\,\delta_{12}e^{-\kappa_B d_2}$ |
| $\mathbf{t}_N^{a_1a_2}=-\big[(1-\alpha_{2A}\alpha_{2B})+\alpha_{A1}\,(\alpha_{2A}-\alpha_{2B})\,\big]e^{-\kappa_A d_1}$ $\mathbf{t}_N^{a_1b_2}=\mathbf{t}_N^{a_1a_2}\alpha_{B3}e^{-\kappa_B d_2}$ | $\mathbf{t}_O^{a_1a_2}=-\alpha_{A1}\,(1-\alpha_{2A}\alpha_{2B})\,\big]e^{-\kappa_A d_1}$ $\mathbf{t}_O^{a_1b_2}=\mathbf{t}_O^{a_1a_2}\alpha_{B3}e^{-\kappa_B d_2}$ $\mathbf{t}_O^{b_1a_2}=-\,(1-\alpha_{2A}\alpha_{2B})$ $\mathbf{t}_O^{b_1b_2}=\mathbf{t}_O^{b_1a_2}\alpha_{B3}e^{-\kappa_B d_2}$ | $\mathbf{t}_P^{b_1a_2}=-\delta_{11}$ $\mathbf{t}_P^{b_1b_2}=\mathbf{t}_P^{b_1a_2}\alpha_{B3}e^{-\kappa_B d_2}$ $\mathbf{t}_P^{a_2a_2}=-\delta_{12}e^{-\kappa_2 a}$ $\mathbf{t}_P^{a_2b_2}=\mathbf{t}_P^{a_1a_2}\alpha_{B3}e^{-\kappa_B d_2}$ |
| $\mathbf{t}_4^{a_1a_2}=-\,(1+\alpha_{2A}\alpha_{A1})\,\delta_{22}e^{-\kappa_A d_1}$ $\mathbf{t}_4^{a_1b_1}=-\,(1+\alpha_{2A}\alpha_{A1})\,\delta_{11}e^{-\kappa_A d_1}e^{\kappa_2 a}$ | $\mathbf{t}_M^{b_1b_1}=-\delta_{12}e^{\kappa_2 a}$ $\mathbf{t}_M^{a_1b_1}=\mathbf{t}_M^{b_1b_2}\alpha_{A1}e^{-\kappa_A d_1}$ $\mathbf{t}_M^{b_1a_2}=-\delta_{22}$ $\mathbf{t}_M^{a_1a_2}=\mathbf{t}_M^{b_1a_2}\alpha_{A1}e^{-\kappa_A d_1}$ | $\mathbf{t}_2^{b_1b_1}=-\delta_{11}\delta_{21}e^{\kappa_2 a}$ $\mathbf{t}_2^{b_1a_2}=-\delta_{11}\delta_{22}$ $\mathbf{t}_2^{a_2b_1}=\mathbf{t}_2^{b_1a_2}$ $\mathbf{t}_2^{a_2b_2}=-\delta_{22}\delta_{12}e^{\kappa_2 a}$ |
| $\mathbf{t}_L^{a_1a_1}=\big[\alpha_{2A}\delta_{22}e^{-\kappa_2 a}-\delta_{21}e^{\kappa_2 a}\big]$ $\mathbf{t}_L^{a_1b_1}=\big[\alpha_{2A}\delta_{21}e^{\kappa_2 a}-\delta_{22}e^{-\kappa_2 a}\big]e^{-\kappa_A d_1}$ | $\mathbf{t}_U^{b_1b_1}=\big[\alpha_{2A}\delta_{21}e^{\kappa_2 a}-\delta_{22}e^{-\kappa_2 a}\big]$ $\mathbf{t}_U^{a_1b_1}=\mathbf{t}_B^{b_1b_1}\alpha_{A1}e^{-\kappa_A d_1}$ $\mathbf{t}_U^{b_1a_1}=\mathbf{t}_B^{a_1b_1}$ $\mathbf{t}_U^{a_1a_1}=\big[\alpha_{2A}\delta_{22}e^{-\kappa_2 a}-\delta_{21}e^{\kappa_2 a}\big]\alpha_{A1}e^{-\kappa_A d_1}$ | $\mathbf{t}_U^{b_1b_1}=-\delta_{12}e^{\kappa_2 a}$ $\mathbf{t}_U^{b_1a_1}=\mathbf{t}_U^{b_2b_1}\alpha_{A1}e^{-\kappa_A d_1}$ $\mathbf{t}_U^{a_2b_1}=-\delta_{22}$ $\mathbf{t}_U^{a_2a_1}=\mathbf{t}_U^{a_2b_1}\alpha_{A1}e^{-\kappa_A d_1}$ |
| $\mathbf{t}_1^{a_1a_1}=\big[\delta_{21}\delta_{11}e^{\kappa_2 a}-\delta_{22}\left(\alpha_{2A}\alpha_{A1}+e^{-2\kappa_A d_1}\right)e^{-\kappa_2 a}\big]$ | $\mathbf{t}_S^{a_1a_1}=\big[\alpha_{2A}\delta_{22}e^{-\kappa_2 a}-\delta_{21}e^{\kappa_2 a}\big]$ $\mathbf{t}_S^{b_1a_1}=\big[\alpha_{2A}\delta_{21}e^{\kappa_2 a}-\delta_{22}e^{-\kappa_2 a}\big]e^{-\kappa_A d_1}$ | $\mathbf{t}_6^{a_2a_1}=-\,(1+\alpha_{2A}\alpha_{A1})\,\delta_{22}e^{-\kappa_A d_1}$ $\mathbf{t}_6^{b_1a_1}=-\,(1+\alpha_{2A}\alpha_{A1})\,\delta_{11}e^{-\kappa_A d_1}e^{\kappa_2 a}$ |

TABLE III. Transition matrix components of five layered dielectric medium scalar electric Green's function–First three columns.

| | |
|---|---|
| $\mathbf{t}_R^{a_2b_2} = \big[\alpha_{2B}\delta_{12}e^{\kappa_2 a} - \delta_{11}e^{-\kappa_2 a})\big]e^{-\kappa_B d_2}$<br>$\mathbf{t}_R^{b_2b_2} = \big[\alpha_{2B}\delta_{11}e^{\kappa_2 a} - \delta_{12}e^{\kappa_2 a}\big]$ | $\mathbf{t}_3^{b_2b_2} = \big[\delta_{21}\delta_{12}e^{\kappa_2 a} - \delta_{11}(\alpha_{2B}\alpha_{B3} + e^{-\kappa_B d_2})e^{\kappa_2 a}\big]$ |
| $\mathbf{t}_B^{a_2a_2} = \big[\alpha_{2B}\delta_{12}e^{\kappa_2 a} - \delta_{11}e^{-\kappa_2 a})\big]$<br>$\mathbf{t}_B^{a_2b_2} = \mathbf{t}_B^{a_2a_2}\alpha_{B3}e^{-\kappa_B d_2}$<br>$\mathbf{t}_B^{b_2a_2} = \mathbf{t}_B^{b_2a_2}$<br>$\mathbf{t}_B^{b_2b_2} = \big[\alpha_{2B}\delta_{11}e^{\kappa_2 a} - \delta_{12}e^{\kappa_2 a}\big]$ | $\mathbf{t}_R^{b_2a_2} = \big[\alpha_{2B}\delta_{12}e^{\kappa_2 a} - \delta_{11}e^{-\kappa_2 a})\big]e^{-\kappa_B d_2}$<br>$\mathbf{t}_R^{b_2b_2} = \big[\alpha_{2B}\delta_{11}e^{\kappa_2 a} - \delta_{12}e^{\kappa_2 a}\big]$ |
| $\mathbf{t}_X^{a_2b_1} = -\delta_{11}$<br>$\mathbf{t}_X^{b_2b_1} = \mathbf{t}_X^{a_2b_1}\alpha_{B3}e^{-\kappa_B d_2}$<br>$\mathbf{t}_X^{a_2a_2} = -\delta_{12}e^{\kappa_2 a}$<br>$\mathbf{t}_X^{b_2a_2} = \mathbf{t}_X^{a_2a_2}\alpha_{B3}e^{-\kappa_B d_2}$ | $\mathbf{t}_9^{b_2b_1} = -\left(1 + \alpha_{2B}\alpha_{B3}\right)\delta_{11}e^{-\kappa_B d_2}$<br>$\mathbf{t}_9^{b_2a_2} = -\left(1 + \alpha_{2B}\alpha_{B3}\right)\delta_{12}e^{-\kappa_B d_2}$ |
| $\mathbf{t}_V^{a_2a_1} = -\alpha_{A1}\left(1 - \alpha_{2A}\alpha_{2B}\right)\big]e^{-\kappa_A d_1}$<br>$\mathbf{t}_V^{b_2a_1} = \mathbf{t}_V^{a_2a_1}\alpha_{B3}e^{-\kappa_B d_2}$<br>$\mathbf{t}_V^{a_2b_1} = -\left(1 - \alpha_{2A}\alpha_{2B}\right)$<br>$\mathbf{t}_V^{b_2b_1} = \mathbf{t}_V^{a_2b_1}\alpha_{B3}e^{-\kappa_B d_2}$ | $\mathbf{t}_W^{b_2b_1} = -\big[\left(1 - \alpha_{2A}\alpha_{2B}\right) + \alpha_{B3}\left(\alpha_{2B} - \alpha_{2A}\right)\big]e^{-\kappa_B d_2}$<br>$\mathbf{t}_W^{b_2a_1} = \mathbf{t}_W^{b_2b_1}\alpha_{A1}e^{-\kappa_A d_1}$ |
| $\mathbf{t}_T^{a_2a_1} = -\big[(1 - \alpha_{2A}\alpha_{2B}) + \alpha_{A1}\left(\alpha_{2A} - \alpha_{2B}\right)\big]e^{-\kappa_A d_1}$<br>$\mathbf{t}_T^{a_1b_2} = \mathbf{t}_T^{a_2a_1}\alpha_{B3}e^{-\kappa_B d_2}$ | $\mathbf{t}_8^{b_2a_1} = \big[(\alpha_{A1} + \alpha_{2A})(\alpha_{2B} + \alpha_{B3})$<br>$-(1 + \alpha_{A1}\alpha_{2A})(1 + \alpha_{2B}\alpha_{B3})\big]e^{-\kappa_A d_1 - \kappa_B d_2}$ |

TABLE IV. Transition matrix components of five layered dielectric medium scalar electric Green's function–last two columns.

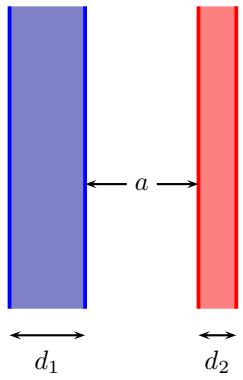


FIG. 7. Two slabs of different thickness. The slabs are infinite in length and breadth.

## IV. INTERACTION ENERGY OF TWO SLABS

Interaction energy between two disjoint obects is given by

$$E_{12} = \frac{1}{2}\int_{-\infty}^{\infty}\frac{d\zeta}{2\pi}\mathrm{Tr}\ln\Big[1-\mathbf{\Gamma}_1 V_1\cdot\mathbf{\Gamma}_2 V_2\Big], \tag{101}$$

where $\mathbf{\Gamma}_i$'s satisfy Eq. (41) with the respective potentials. Parallel slabs are described by the potentials

$$V_i(z) = (\varepsilon_i - 1)\left[\theta(z-a_i) - \theta(z-b_i)\right], \qquad i = 1, 2, \tag{102}$$

where $b_i - a_i = d_i$ are the thickness' of slabs, and $a_2 - b_1 = a$ is the distance between the slabs (see FIG. 7). Using translational symmetry we can write the Casimir energy per unit area for parallel slabs in the form

$$\mathcal{E}(a, d_i, \varepsilon_i - 1) = \frac{E_{12}}{L_x L_y} = \frac{1}{2}\int_{-\infty}^{\infty}\frac{d\zeta}{2\pi}\int\frac{d^2k}{(2\pi)^2}\,\mathrm{tr}\ln\Big[1-\mathbf{K}(i\zeta,k)\Big], \tag{103}$$

where trace is now only over the dyadic indices. The dyadic $\mathbf{K}(i\zeta,k)$ is given in terms of the reduced Green's dyadic in Eq. (75) as

$$\mathbf{K}(i\zeta,k) = (\varepsilon_1-1)(\varepsilon_2-1)\int_{a_1}^{b_1}dz\int_{a_2}^{b_2}dz'\boldsymbol{\gamma}_{1⑨}(z',z;i\zeta,k)\cdot\boldsymbol{\gamma}_{2④}(z,z';i\zeta,k), \tag{104}$$

where the circled number in the subscript denotes the particular region in FIG. 4 in which the dyadic is to be evaluated. The reduced Greeen's dyadic are given in terms of electric and magnetic Green's functions in Eqs. (68a) and (68b), whose solutions, for parallel slabs described by the potentials in Eq. (102), are given in Eq. (89). The region of evaluation is unambiguously specified by the integration regions. The solution for the Green's dyadic for an individual plate is unaware of the presence of the other plate. Thus the meshed regions in Figure 8 belongs to the solid (blue) lines, which according to Figure 4 corresponds to region 9 for the first slab and region 4 for the second slab. The solution to the reduced electric Green's dyadic is given by Eq. (75). Notice that we can omit the $\delta$-function term since $z$ and $z'$ are never evaluated at the same point.

Due to the particular dyadic structure of the dimensionally reduced Green's dyadic in Eq. (75) we observe the factorization

$$\Big[\mathbf{1}-\mathbf{K}(i\zeta,k)\Big] = \Big[1-K^E(\mathbf{x},i\zeta)\Big]\Big[\mathbf{1}-\mathbf{K}^H(i\zeta,k)\Big], \tag{105}$$

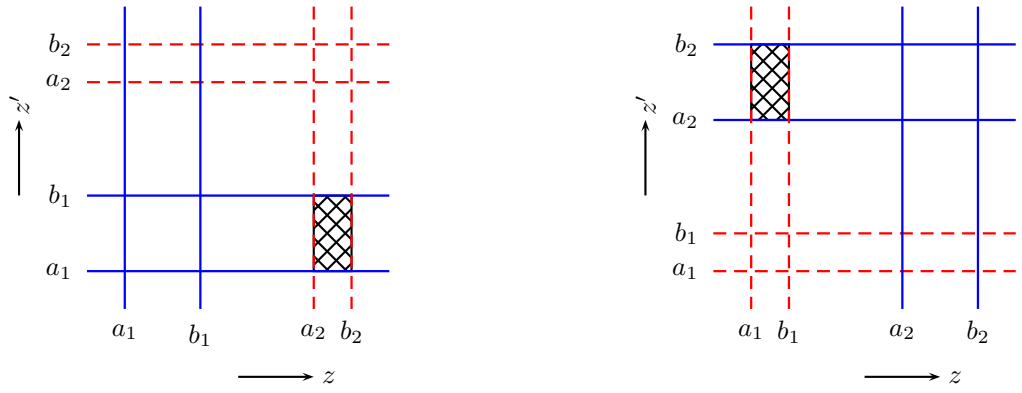


FIG. 8. Region of integration for $\boldsymbol{\gamma}_1(z,z')$ (left) and $\boldsymbol{\gamma}_2(z,z')$ (right) in Eq. (104) shown as crosshatched.

where

$$K^E(i\zeta,k) = (\varepsilon_1-1)(\varepsilon_2-1)\zeta^4 \int_{a_1}^{b_1} dz \int_{a_2}^{b_2} dz'\, g^E_{1⑨}(z',z;i\zeta,k) g^E_{2④}(z,z';i\zeta,k), \tag{106}$$

$$\mathbf{K}^H(i\zeta,k) = (\varepsilon_1-1)(\varepsilon_2-1) \int_{a_1}^{b_1} dz \int_{a_2}^{b_2} dz'\, \boldsymbol{\gamma}^H_{1⑨}(z',z;i\zeta,k) \cdot \boldsymbol{\gamma}^H_{2④}(z,z';i\zeta,k). \tag{107}$$

This leads to the decomposition of the interaction energy into electric and magnetic parts in the form

$$\mathcal{E}(a,d_i,\varepsilon_i-1) = \frac{1}{2}\int_{-\infty}^{\infty}\frac{d\zeta}{2\pi}\int\frac{d^2k}{(2\pi)^2}\left\{\ln\left[1-K^E(i\zeta,k)\right] + \operatorname{tr}\ln\left[1-\mathbf{K}^H(i\zeta,k)\right]\right\}. \tag{108}$$

The dimensionally reduced Green's dyadics are

$$\boldsymbol{\gamma}^H_{1⑨}(z',z;i\zeta,k) = \frac{1}{\varepsilon_1}\begin{bmatrix} \frac{\partial}{\partial z'}\frac{\partial}{\partial z} g^H_{1⑨}(z',z) & ik\frac{\partial}{\partial z'} g^H_{1⑨}(z',z) \\ -ik\frac{\partial}{\partial z} g^H_{1⑨}(z',z) & k^2 g^H_{1⑨}(z',z) \end{bmatrix} \tag{109}$$

where we have used the fact that in region 9 (see FIG. 4 and FIG. 8)

$$\varepsilon_1(z)\to\varepsilon_1, \qquad \varepsilon_1(z')\to 1. \tag{110}$$

The $\delta$-function term in Eq. (75) does not contribute. Similarly

$$\boldsymbol{\gamma}^H_{2④}(z,z';i\zeta,k) = \frac{1}{\varepsilon_2}\begin{bmatrix} \frac{\partial}{\partial z}\frac{\partial}{\partial z'} g^H_{2④}(z,z') & ik\frac{\partial}{\partial z} g^H_{2④}(z,z') \\ -ik\frac{\partial}{\partial z'} g^H_{2④}(z,z') & k^2 g^H_{2④}(z,z') \end{bmatrix} \tag{111}$$

where we have used the fact that in region 4 (see FIG. 4 and FIG. 8)

$$\varepsilon_2(z)\to 1, \qquad \varepsilon_2(z')\to\varepsilon_2. \tag{112}$$

Using Eqs. (110) and (112) in the equation for the magnetic Green's function in Eq. (68b) we have

$$\frac{\partial}{\partial z'} g^H_{1⑨}(z',z) = -\kappa g^H_{1⑨}(z',z), \qquad \frac{\partial^2}{\partial z'^2} g^H_{1⑨}(z',z) = \kappa^2 g^H_{1⑨}(z',z), \tag{113a}$$

$$\frac{\partial}{\partial z} g^H_{2④}(z,z') = -\kappa g^H_{2④}(z,z'), \qquad \frac{\partial^2}{\partial z^2} g^H_{2④}(z,z') = \kappa^2 g^H_{2④}(z,z'). \tag{113b}$$

Multiplying the two dyadics, and using Eqs. (113) to simplify the resulting expression, we obtain

$$\mathbf{K}^H(i\zeta,k) = \begin{bmatrix} K^H_{11}(i\zeta,k) & K^H_{13}(i\zeta,k) \\ K^H_{31}(i\zeta,k) & K^H_{33}(i\zeta,k) \end{bmatrix}, \tag{114}$$

whose components are:

$$K^H_{11}(i\zeta,k) = \frac{(\varepsilon_1-1)}{\varepsilon_1}\frac{(\varepsilon_2-1)}{\varepsilon_2}\int_{a_1}^{b_1} dz \int_{a_2}^{b_2} dz' \left[\kappa^2\zeta^2 - \kappa^3\frac{\partial}{\partial z} + \kappa\zeta^2\frac{\partial}{\partial z'} - \kappa^2\frac{\partial}{\partial z}\frac{\partial}{\partial z'}\right] g^H_{1⑨}(z',z) g^H_{2④}(z,z'), \tag{115a}$$

$$K^H_{33}(i\zeta,k) = \frac{(\varepsilon_1-1)}{\varepsilon_1}\frac{(\varepsilon_2-1)}{\varepsilon_2}\int_{a_1}^{b_1} dz \int_{a_2}^{b_2} dz' \left[-k^2\zeta^2 + k^2\kappa\frac{\partial}{\partial z}\right] g^H_{1⑨}(z',z) g^H_{2④}(z,z'), \tag{115b}$$

$$K^H_{13}(i\zeta,k) = -\frac{(ik\kappa)}{k^2}\, K^H_{33}(i\zeta,k), \tag{115c}$$

$$K^H_{31}(i\zeta,k) = \frac{(ik\kappa)}{\kappa^2}\, K^H_{11}(i\zeta,k). \tag{115d}$$

Using the above we can derive

$$\det K^H(i\zeta,k) = 0, \tag{116}$$

which imples

$$\text{tr ln}\left[1 - \mathbf{K}^H(i\zeta,k)\right] = \ln\left[1 - \text{tr}\,\mathbf{K}^H(i\zeta,k)\right]. \tag{117}$$

Further,

$$\text{tr}\,\mathbf{K}^H(i\zeta,k) = \frac{(\varepsilon_1-1)}{\varepsilon_1}\frac{(\varepsilon_2-1)}{\varepsilon_2}\zeta^4\int_{a_1}^{b_1} dz \int_{a_2}^{b_2} dz' \left(1 - \frac{\kappa}{\zeta^2}\frac{\partial}{\partial z}\right)\left(1 + \frac{\kappa}{\zeta^2}\frac{\partial}{\partial z'}\right) g^H_{1⑨}(z',z) g^H_{2④}(z,z'). \tag{118}$$

### A. Casimir energy for two slabs

For clarity and convenience we isolate the evaluation into stages. The relevant region-specific Green's functions, using Eq. (89), are

$$g^E_{1⑨}(z_2,z_1;i\zeta,k) = \frac{1}{(1-\alpha_1^2 e^{-2\kappa_1 d_1})}\frac{1}{(\kappa_1+\kappa)}\, e^{-\kappa(z_2-b_1)}\left[e^{-\kappa_1(b_1-z_1)} + \alpha_1 e^{-\kappa_1 d_1} e^{-\kappa_1(z_1-a_1)}\right], \tag{119a}$$

$$g^E_{2④}(z_1,z_2;i\zeta,k) = \frac{1}{(1-\alpha_2^2 e^{-2\kappa_2 d_2})}\frac{1}{(\kappa_2+\kappa)}\, e^{-\kappa(a_2-z_1)}\left[e^{-\kappa_2(z_2-a_2)} + \alpha_2 e^{-\kappa_2 d_2} e^{-\kappa_2(b_2-z_2)}\right], \tag{119b}$$

where $\kappa_i$'s and $\alpha_i$'s are defined as

$$\kappa_i^2 = k^2 + \zeta^2\varepsilon_i = \kappa^2 + \zeta^2(\varepsilon_i - 1), \qquad \text{and} \qquad \alpha_i = \frac{\kappa_i - \kappa}{\kappa_i + \kappa}. \tag{120}$$

The corresponding magnetic Green's functions are obtained from the electric Green's functions by the replacement

$$\kappa_i \to \bar\kappa = \frac{\kappa_i}{\varepsilon_i} \tag{121}$$

everywhere except in the exponentials.

Using the Green's functions we can write

$$K^E(i\zeta,k) = t_1^E(i\zeta,k)\, t_2^E(i\zeta,k)\, e^{-2\kappa a}, \tag{122a}$$

$$\text{tr}\,\mathbf{K}^H(i\zeta,k) = t_1^H(i\zeta,k)\, t_2^H(i\zeta,k)\, e^{-2\kappa a}, \tag{122b}$$

where

$$t_i^E(i\zeta,k) = \frac{e^{\kappa a}}{(1-\alpha_i^2 e^{-2\kappa_i d_i})}\frac{(\varepsilon_i-1)\zeta^2}{(\kappa_i+\kappa)}\int_{a_i}^{b_i} dz\, u_i^E(z), \tag{123a}$$

$$t_i^H(i\zeta,k) = \frac{e^{\kappa a}}{(1-\bar\alpha_i^2 e^{-2\kappa_i d_i})}\frac{(\varepsilon_i-1)\zeta^2}{\varepsilon(\bar\kappa_i+\kappa)}\int_{a_i}^{b_i} dz \left[1 + (-1)^i\frac{\kappa}{\zeta^2}\frac{\partial}{\partial z}\right] u_i^H(z), \tag{123b}$$

where

$$u_1^E(z) = e^{-\kappa(a_2-z)}\left[e^{-\kappa_1(b_1-z)} + \alpha_1 e^{-\kappa_1 d_1} e^{-\kappa_1(z-a_1)}\right], \tag{124a}$$

$$u_2^E(z) = e^{-\kappa(z-b_1)}\left[e^{-\kappa_2(z-a_2)} + \alpha_2 e^{-\kappa_2 d_2} e^{-\kappa_2(b_2-z)}\right]. \tag{124b}$$

The functions $u_i^H(z)$ are given in terms of $u_1^E(z)$ as

$$u_i^H(z) = \bar{u}_i^E(z), \tag{125}$$

Completing the $z$-integral in Eq. (123a) and using the definition of $\kappa_i$ to replace $(\varepsilon_i - 1)\zeta^2$ we derive

$$t_i^E(i\zeta, k) = \frac{\alpha_i}{\Delta_i}, \qquad i = 1, 2, \tag{126}$$

where the determinants $\Delta_i$'s are

$$\frac{1}{\Delta_i} = \frac{(1 - e^{-2\kappa_i d_i})}{(1 - \alpha_i^2 e^{-2\kappa_i d_i})}, \tag{127}$$

Repeating the procedure in Eq. (123b) and using the identity

$$k^2 \pm \kappa\kappa_i = -\zeta^2 \varepsilon_i \frac{(\bar{\kappa}_i \mp \kappa)}{(\kappa_i \mp \kappa)}, \tag{128}$$

we derive

$$t_i^H(i\zeta, k) = \bar{t}_i^E(i\zeta, k). \tag{129}$$

Thus we have the Casimir interaction energy between parallel slabs to be

$$\mathcal{E}(a, d_i, \varepsilon_i - 1) = \frac{1}{2}\int_{-\infty}^{\infty} \frac{d\zeta}{2\pi} \int \frac{d^2k}{(2\pi)^2} \left\{ \ln\left[1 - t_1^E(i\zeta, k)\, t_2^E(i\zeta, k)\, e^{-2\kappa a}\right] + \ln\left[1 - t_1^H(i\zeta, k)\, t_2^H(i\zeta, k)\, e^{-2\kappa a}\right] \right\}. \tag{130}$$

It is instructive to note that the dependence in the properties of the individual plates is inside $t_i^E$ and $t_i^H$. More explicitly we have

$$t_i^{E,H}(i\zeta, k) \to t_i^{E,H}(i\zeta, k; d_i, \varepsilon_i - 1). \tag{131}$$

### 1. *Lifshitz energy for two infinite dielectric semi-spaces*

We can obtain the standard Lifshitz result [18] by taking the thick-plate limit ($d_i \to \infty$). In this case we have $\Delta_i^N \to 1$ and $\bar{\Delta}_i^N \to 1$. Thus

$$t_i^E(i\zeta, k; \infty, \varepsilon_i - 1) = \alpha_i, \qquad t_i^H(i\zeta, k; \infty, \varepsilon_i - 1) = \bar{\alpha}_i. \tag{132}$$

Using this in Eq. (130) we get

$$\mathcal{E}(a, \infty, \varepsilon_i - 1) = \frac{1}{2}\int_{-\infty}^{\infty} \frac{d\zeta}{2\pi} \int \frac{d^2k}{(2\pi)^2} \left\{ \ln\left[1 - \alpha_1\, \alpha_2\, e^{-2\kappa a}\right] + \ln\left[1 - \bar{\alpha}_1\, \bar{\alpha}_2\, e^{-2\kappa a}\right] \right\}. \tag{133}$$

Here $\alpha_i$ and $\bar{\alpha}_i$ are the reflection coefficients $r_{\rm TE}$ and $r_{\rm TM}$ used in the literature.

### 2. *Casimir energy for two perfectly conducting plates*

It is straightforward to obtain the classic Casimir energy for the two perfectly conducting plates from either Eq. (132) or Eq. (133). For a perfect conductor we take the limit ($\varepsilon_i \to \infty$), for which we have $\alpha_i \to 1$, $\bar{\alpha}_i \to -1$, $\Delta_i^N \to 1$ and $\bar{\Delta}_i^N \to 1$,

$$t_i^E(i\zeta, k; d_i, \infty) = 1, \qquad t_i^H(i\zeta, k; d_i, \infty) = -1. \tag{134}$$

This leads to

$$\begin{aligned} \mathcal{E}(a, d_i, \infty) &= \frac{1}{2}\int_{-\infty}^{\infty} \frac{d\zeta}{2\pi} \int \frac{d^2k}{(2\pi)^2}\, 2\, \ln\left[1 - e^{-2\kappa a}\right] \\ &= \frac{1}{2\pi^2}\int_0^{\infty} \kappa^2 d\kappa \ln\left[1 - e^{-2\kappa a}\right] \\ &= -\frac{\pi^2}{720\, a^3}. \end{aligned} \tag{135a}$$

The above result is true without necessarily taking the thick-plate limit, which amounts to saying that in the perfect conductor limit the only region of interest is the space in between the slabs since the fields are zero inside the perfect conductor.

### 3. van der Waals interaction energy between two slabs

In the dilute dielectric limit ($\varepsilon_i - 1 \ll 1$), which is also the van der Waals limit, we have

$$t_i^E(i\zeta, k; d_i, \varepsilon_i - 1) \sim (\varepsilon_i - 1)(1 - e^{-2\kappa d_i})\frac{\zeta^2}{4\kappa^2}, \tag{136}$$

$$t_i^H(i\zeta, k; d_i, \varepsilon_i - 1) \sim (\varepsilon_i - 1)(1 - e^{-2\kappa d_i})\left[\frac{\zeta^2}{4\kappa^2} - \frac{1}{2}\right]. \tag{137}$$

This leads to van der Waals energy between two slabs given by

$$\begin{aligned}\mathcal{E}(a, d_i, \varepsilon_i - 1) &= -\frac{(\varepsilon_1 - 1)(\varepsilon_2 - 1)}{256\,\pi^3}\int_{-\infty}^{\infty}\frac{d\zeta}{2\pi}\int_{-\infty}^{\infty}\frac{dk_x}{2\pi}\int_{-\infty}^{\infty}\frac{dk_y}{2\pi}(1 - e^{-2\kappa d_1})(1 - e^{-2\kappa d_2})\,e^{-2\kappa a}\left[\frac{\zeta^4}{\kappa^4} + \frac{(\zeta^2 - 2\kappa^2)^2}{\kappa^4}\right] \\ &= -\frac{1}{3}\frac{23\,(\varepsilon_1 - 1)(\varepsilon_2 - 1)}{1920\,\pi^2}\frac{1}{2}\frac{\partial^3}{\partial a^3}\ln\left[\frac{a(a + d_1 + d_2)}{(a + d_1)(a + d_2)}\right] + \mathcal{O}(\varepsilon_i - 1)^2,\end{aligned} \tag{138}$$

where the superscript on $(\varepsilon_i - 1)$ on the left hand side signifies that the expression is in the leading order approximation in $(\varepsilon_i - 1)$. In the thick plate limit the above expression leads to the classic van der Waals interaction energy between two thick slabs as

$$\mathcal{E}(a, \infty, \varepsilon_i - 1) = -\frac{1}{3}\frac{23\,(\varepsilon_1 - 1)(\varepsilon_2 - 1)}{640\,\pi^2\,a^3} + \mathcal{O}(\varepsilon_i - 1)^2. \tag{139}$$

## V. DIELECTRIC MODELS FOR THIN PLATES

In our calculation the background potentials describing the objects are modelled by the dielectric permittivity $\varepsilon(\omega)$ of the material objects. The response of the system in terms of polarization of the medium to an applied electric field is given by Eq. (3), which in the frequency domain reads

$$\mathbf{P}(\omega) = [\varepsilon(\omega) - 1]\mathbf{E}(\omega). \tag{140}$$

This is a macroscopic effect which is constructed out of the microscopic dipole moments of individual atoms. Thus,

$$\mathbf{P} = ne\bar{\mathbf{x}}, \tag{141}$$

where $\bar{\mathbf{x}}$ is the average of the positions of individual atoms with respect to the center of mass of the material. (The position of the center of mass does not contribute at the macroscopic level if the material is neutral in charge.) $n$ in the above expression is the number density and prescribes the process of statistical averaging. The individual response at the microscopic level is modelled by studying the motion of a single charge inside a material medium. An extremely successful model is the Drude-Lorentz model

$$m\left[\frac{d^2}{dt^2} + \gamma\frac{d}{dt} + \omega_0^2\right]\mathbf{x} = e\mathbf{E} \tag{142}$$

in which the charge is bound to the atom by an oscillator force parametrized by $\omega_0$ and the effects of collisions with other atoms are collected in the dissipation term parametrized by $\gamma$. In the frequency space we then have

$$\mathbf{x} = \frac{e}{m}\left[\frac{1}{\omega_0^2 - \omega^2 - i\omega\gamma}\right]\mathbf{E}. \tag{143}$$

Combining Eqs. (140), (141), and (143) we have the Drude-Lorentz dielectric model for the dielectric permittivity

$$\varepsilon(\omega) - 1 = \frac{\omega_{f/b}^2}{\omega_0^2 - \omega^2 - i\omega\gamma}, \qquad \omega_{f/b}^2 = n_{f/b}\frac{e^2}{m}, \tag{144}$$

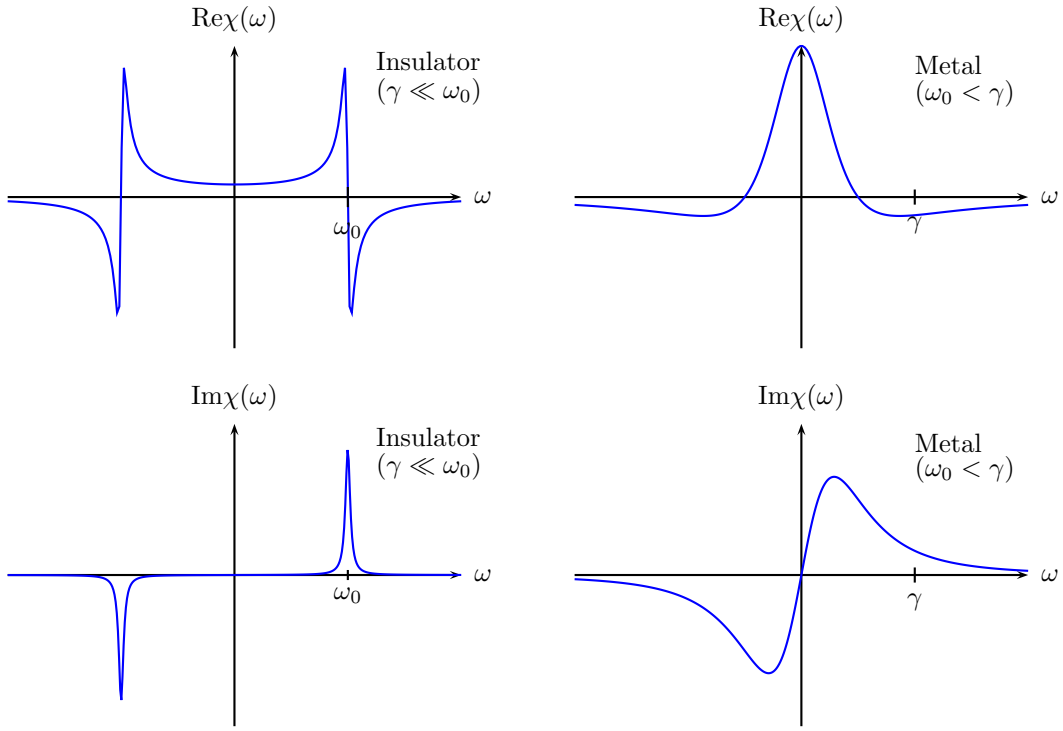


FIG. 9. Dielectric properties of an insulator and metal described by Drude-Lorentz model

where $\omega_{f/b}$ is given in terms of number density of free charges $n_f$ or bound charges $n_b$. For cases when $\omega_0 \gg \gamma$ the model represents an insulator, and for $\omega_0 \ll \gamma$ it represents metals. It is called the Drude model when $\omega_0 = 0$, which was originally proposed by Drude in 1900. Later it was gerneralized by Lorentz in 1905. Langevin-Debye model in 1912 extended the Drude-Lorentz model to describe materials with polar molecules (eg. water). Sommerfeld in 1933 using Fermi-Dirac distribution for the number density in Eq. (141) in conjunction with the Drude-Lorentz model successfully explained the specific heat of metals.

Real and imaginary parts of the dielectric function described by the Drude-Lorentz model are plotted for typical insulator and metal in FIG. 9. Real part of the dielectric function (square of refractive index) represents dispersion and anamolous dispersion is the behaviour when the refractive index decreases with increase in frequency. Imaginary part of the dielectric function represents absorption. The plots show that anamoulous dispersion is accompanied by absorption. Refractive index, reflectivity, absorption, and transmittance, are all given in terms of the dielectric function. For example, inside the frequency regime of anamolous dispersion if dissipation is negligible ($\gamma = 0$) light of certain frequency is totally reflected. In the presence of damping light is partially reflected and partially absorbed. We found Sernelius' survey of these concepts in [19] useful.

In the regime where both $\omega_0$ and $\gamma$ are negligible and can be set to zero we have the plasma model

$$\varepsilon(\omega) - 1 = -\frac{\omega_p^2}{\omega^2}, \tag{145}$$

in which the bound charges do not contribute because they are inert due to their high nertia in such high frequency regimes. The above equation seems to indicate $\varepsilon(\omega) < 1$, which might naively lead to violate causality, but we refer to chapter 7 of [3] for a discussion on how Eq. (145) is compatible with causality.

For materials in which the dissipation term dominates we have the conductor model

$$\varepsilon(\omega) - 1 = i\frac{\sigma}{\omega}, \qquad \sigma = \frac{\omega_f^2}{\gamma}, \tag{146}$$

where $\sigma$ is the conductivity in the material. Dissipation of electromagnetic energy in a relativistic theory is described by the so-called vacuum polarization diagram. Thus, in a conductor in which the electrons are typically non-relativistic dissipation is expected to be described by the analogous vacuum polarization diagram.

The plasma frequency for a metal in the non-quantum regime is defined as

$$[\omega_p(\infty)]^2 = \frac{e^2}{m} n_f(\infty). \tag{147}$$

The $\infty$ in the parenthesis denote the non-quantum regime, and the parameter representing the transition from classical to quantum will be introduced in the following. Drude-Lorentz model uses the classical number density, $n_f(\infty)$. Sommerfeld revised the Drude-Lorentz model by using Fermi-Dirac distribution to calculate $n_f$ which we shall call the Drude-Lorentz-Sommerfeld (DLS) model. In the DLS model the conduction electrons inside a metal are modelled as a gas. The conduction electrons are assumed to be not interacting with each other.

### *4. Number density*

To describe the electrons (in the electron gas) in a slab, we consider the energy states of a particle confined in a slab of thickness $d$ and infinite in extent along the $x$-$y$ directions using the Schrödinger equation

$$-\frac{\hbar^2}{2m}\left[\frac{\partial^2}{\partial x^2}+\frac{\partial^2}{\partial y^2}+\frac{\partial^2}{\partial z^2}\right]\psi(x,y,z) = E\psi(x,y,z). \tag{148}$$

The confinement of the particle inside the slab requires the proability flux to be zero on the walls,

$$\frac{\partial}{\partial z}\psi^*\psi\bigg|_{z=0,d} = \left[\psi^*\left(\frac{\partial}{\partial z}\psi\right)+\left(\frac{\partial}{\partial z}\psi^*\right)\psi\right]\bigg|_{z=0,d} = 0. \tag{149}$$

The above condition can be satisfied by either requiring Dirichlet boundary condition ($\psi = 0$), or requiring Neumann boundary condition ($\partial\psi/\partial z = 0$) on the wavefunction at the walls. But, Dirichlet boundary conditions are over-imposing because it does not allow surface charges on the slabs. Thus, we rule out Dirichlet boundary condition and impose Neumann boundary condition on the particles. Fourier transforming in the $x$-$y$ directions we have

$$E_n(k_x,k_y) = \frac{\hbar^2}{2m^*}\left[k_x^2+k_y^2+n^2\frac{\pi^2}{d^2}\right], \qquad n = 0,1,2,\ldots. \tag{150}$$

Unlike Dirichlet condition $n = 0$ state is not excluded when Neumann boundary conditions are imposed.

The total number of electrons in the slab is equal to twice the sum of occupied energy levels. In terms of the maximum occupied energy level at zero temperature, termed Fermi energy $E_F$, we can thus write

$$n_f = \frac{n_{\rm tot}(E_F)}{L_xL_yd} = 2\,\frac{1}{d}\sum_{n=0}^{\infty}\int_{-\infty}^{\infty}\frac{dk_x}{2\pi}\int_{-\infty}^{\infty}\frac{dk_y}{2\pi}\,\theta(E_F-E_n(k_x,k_y)), \tag{151}$$

where the factor of 2 accomodates two electrons in each state. Observing the facorization

$$\theta(a-x-y) = \theta(a-x-y)\theta(a-x) \tag{152}$$

allows the separation of the variables in the form

$$n_f = \frac{n_{\rm tot}(E_F)}{L_xL_yd} = 2\,\frac{1}{d}\sum_{n=0}^{\infty}\theta\left(E_F-n^2\frac{\hbar^2}{2m}\frac{\pi^2}{d^2}\right)\int_{-\infty}^{\infty}\frac{dk_x}{2\pi}\int_{-\infty}^{\infty}\frac{dk_y}{2\pi}\theta\left(E_F-\frac{\hbar^2}{2m}k^2-n^2\frac{\hbar^2}{2m}\frac{\pi^2}{d^2}\right) \tag{153}$$

$$= \frac{1}{2\pi d}\sum_{n=0}^{\infty}\theta\left(E_F-n^2\frac{\hbar^2}{2m}\frac{\pi^2}{d^2}\right)\left[\frac{2mE_f}{\hbar^2}-n^2\frac{\pi^2}{d^2}\right] \tag{154}$$

$$= \frac{\pi}{2d^3}\sum_{n=0}^{\infty}(N^2-n^2)\theta(N^2-n^2) = \frac{\pi}{2d^3}\sum_{n=0}^{[N]}(N^2-n^2), \tag{155}$$

where $[N]$ is the integer part of

$$N = \sqrt{\frac{2m^*E_Fd^2}{\hbar^2\pi^2}} = \frac{k_Fd}{\pi} = \frac{2d}{\lambda_F}, \tag{156}$$

and expressed in terms of Fermi wave-vector, $k_F$, and Fermi wavelength, $\lambda_F$. Using the sums

$$\sum_{n=0}^{[N]} N^2 = N^2([N]+1), \qquad \sum_{n=0}^{[N]} n^2 = \frac{1}{6}[N]([N]+1)(2[N]+1), \tag{157}$$

we immediately have

$$n_f(N) = \frac{\pi}{2d^3}\left[\left([N]N^2 - \frac{1}{3}[N]^3\right) + \left(N^2 - \frac{1}{2}[N]^2\right) - \frac{1}{6}[N]\right], \tag{158}$$

For metals described by the DLS model the Fermi wavelength ranges between 0.3 nm - 1 nm. Notice that the limit $\hbar \to 0$ is equivalent to taking $k_F \to \infty$ ($N \to \infty$). The number density in the limit $N \to \infty$ is

$$n_f(\infty) = \frac{\pi}{2d^3}\frac{2}{3}N^3 = \frac{k_F^3}{3\pi^2}. \tag{159}$$

Using Eq. (159) in Eq. (158) we have

$$n_f(N) = n_f(\infty)\nu(x), \tag{160}$$

where

$$\nu(x) = \frac{3}{2}\left(x - \frac{1}{3}x^3\right) + \frac{3}{2N}\left(1 - \frac{1}{2}x^2\right) - \frac{1}{4N^2}x, \qquad x = \frac{[N]}{N}. \tag{161}$$

We note the limiting cases (see FIG. 10)

$$x = \frac{[N]}{N} \to \begin{cases} 0 & \text{if} \quad N < 1, \\ 1 & \text{if} \quad N \to \infty. \end{cases} \tag{162}$$

Convergence of $x$ to unity is very slow. In particular we make an error of 1% in replacing $x \to 1$ even for N=100. The limiting cases for $\nu(x)$ in Eq. (161) are:

$$\nu(x) \to \begin{cases} \frac{3}{2N} & \text{if} \quad N < 1, \\ 1 & \text{if} \quad N \to \infty. \end{cases} \tag{163}$$

Using Eq. (163) we have the following limiting expressions for the number density in Eq. (160):

$$n_f(N) \to n_f(\infty)\left\{ \begin{array}{c} \frac{3}{2N} \\ 1 \end{array} \right\} = \begin{cases} \frac{k_F^2}{2\pi d} & \text{if} \quad N < 1 \ (2d < \lambda_F), \\ \frac{k_F^3}{2\pi^2} & \text{if} \quad N \to \infty \ (2d \gg \lambda_F). \end{cases} \tag{164}$$

### *5. de-Haas–van Alphen effect*

The third term inside the square bracket on the right hand side of Eq. (150) exhibits the discretization of the Fourier modes due to confinement. Energy of a charged particle in the presence of a magnetic field also involves an analogous discretization

$$E_n^{\text{mag}}(k_x, k_y) = \frac{\hbar^2}{2m^*}\left[k_x^2 + k_y^2 + n^2\frac{2eB}{\hbar c}\right], \qquad n = 0, 1, 2, \ldots, \tag{165}$$

which is the famous Landau quantization. Comparison of Eqs. (150) and (165) suggests the following correspondence between quantum thin plate effects and the quantization effects due to the presence of magnetic field:

$$\frac{d^2}{\pi^2} \leftrightarrow \frac{\hbar c}{2eB}. \tag{166}$$

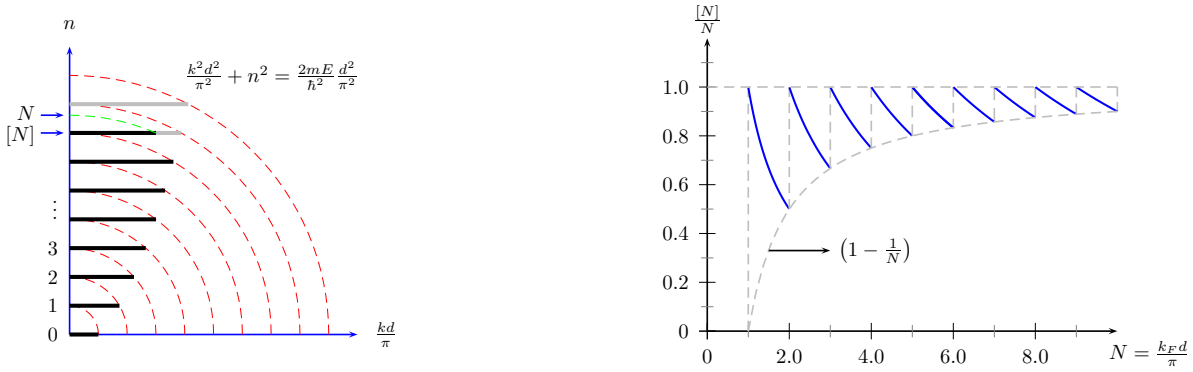


FIG. 10. Left: Energy filling scheme and description of $[N]$ and $N$. Right: Fractional Floor function $\frac{[N]}{N}$ plotted with respect to $N$.

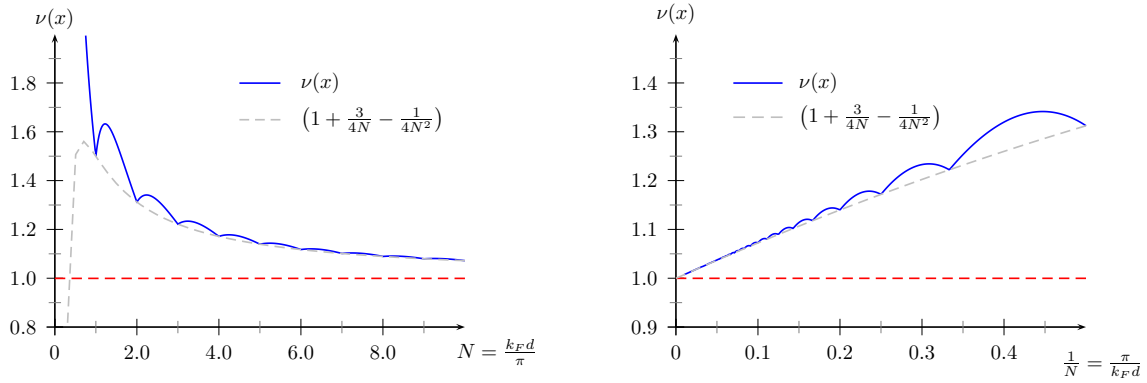


FIG. 11. Plot of $\nu(x)$ versus $N$ (on left) and versus $\frac{1}{N}$ (on right).

Note the appearance of $\hbar c$ in this analogy.

de-Haas and van-Alphen in 1930 experimentally measured the magnetization of a sample of bismuth as a function of high magnetic field at relatively low temperatures, and found oscillations in the plot. The interpretation of these oscillations was given by Onsager in 1952. These oscillations were predicted by Landau in 1930 without being aware of the experiment [20]. This phenomenon which is a signature of quantum mechanical effect has been observed in measurements of various other physical quantities [21]. de-Haas–van Alphen effect is used to probe the Fermi surface of a material and to measure the number density.

The oscillations in the function $\nu(x)$, see Eq. (161), plotted in FIG. 11, are the source of de-Haas–van Alphen oscillations. For comparison refer to Figure 14.3 in [21].

### 6. *Plasma frequency*

Using Eq. (164) in Eq. (147) we have the quantum correction to plasma frequency due to finite thickness of the plate to be

$$[\omega_p(N)]^2 = [\omega_p(\infty)]^2 \nu(x) \to [\omega_p(\infty)]^2 \begin{cases} \frac{3}{2N} & \text{if} \quad N < 1 \ (2d < \lambda_F), \\ 1 & \text{if} \quad N \to \infty \ (2d \gg \lambda_F), \end{cases} \tag{167}$$

where $\omega_p(\infty)$ was introduced in Eq. (147). This can be rewritten in the form (using Eq. (159))

$$[\omega_p(\infty)]^2 = \left[\frac{e^2}{m^* c^3}\right](ck_F)^3, \tag{168}$$

where we have replaced the mass with an effective mass $m^*$ to convey that the plasma frequency is in general independent of the Fermi momentum. The effective mass typically varies between $0.01\,m$ to $10\,m$ for materials.

In graphene near the so called Dirac points the effective mass is zero at zero temperature and about $m/18$ at room temperature. For typical metals the plasma frequency, $\omega_p(\infty)$, is between $(1-7)\times 10^{15}$ rad/s, and the Fermi momentum, $ck_F$ is between $(1-6)\times 10^{18}$ rad/s. It is suggestive to introduce the thickness inside the effective mass to write

$$m^* = \frac{m}{\nu(x)} \tag{169}$$

as a consequence of Eq. (167).

In the following we shall find it suitable to introduce the parameter

$$u_p = \frac{\omega_p(\infty)}{ck_F} \tag{170}$$

representing the empirical relation between the plasma frequency and Fermi momentum. For typical metals $u_p = 10^{-3}$.

## VI. CASIMIR ENERGY FOR THIN PLATES

We shall limit our discussion to plasma models to reduce the number of parameters minimal in the discussion. Casimir energy between slabs described by the plasma model is given by Eq. (130) in conjunction with Eq. (145),

$$\mathcal{E}(a, d_i, \varepsilon_i - 1) \to \mathcal{E}_L(a, d_i; \omega_{pi}(\infty)), \tag{171}$$

where the subscript stands for Lifshitz even though the above expression is generalized to be applicable for slabs of finite thickness. The parameter $\omega_{pi}(\infty)$ describes the dielectic function $(\varepsilon_i - 1)$ for the plasma model.

Sommerfeld's revision is instated in the model by the replacement

$$\omega_{pi}(\infty) \to \omega_{pi}(N) \tag{172}$$

in Eq. (171) using Eq. (167), which leads to the expression for the Casimir energy between slabs as

$$\mathcal{E}_L(a, d_i; \omega_{pi}(\infty)) \to \mathcal{E}_P(a, d_i; \omega_{pi}(N)), \tag{173}$$

where the subscript now stands for 'plates' with the oversight that we will use 'TP' for thin plates.

Fermi energy introduces a model dependent scale in the problem. Plasma model is parametrized by $\omega_{pi}$ and $k_F$ which lets us write

$$\mathcal{E}_P(a, d_i; \omega_{pi}(N)) \to \mathcal{E}_P(a, d_i; \omega_{pi}(\infty), k_F). \tag{174}$$

Since $\omega_{pi}(N) \to \omega_{pi}(\infty)$ in the limit $k_F \to \infty$, we conclude that the classical expression for the Casimir energy between two slabs given by $\mathcal{E}_L(a, d_i; \omega_{pi}(\infty))$ is obtained by taking $k_F \to \infty$ in the generalized expression. Thus we have the relation

$$\lim_{k_F \to \infty} \mathcal{E}_P(a, d_i; \omega_{pi}(\infty), k_F) = \mathcal{E}_L(a, d_i; \omega_{pi}(\infty)). \tag{175}$$

We choose the Fermi momentum to set the scale in the problem by fixing $k_F = 1$. This leads to the following redefinition of the parameters

$$\mathcal{E}_P(a, d_i; \omega_{pi}(\infty), k_{Fi}) \to \mathcal{E}_P(k_F a, N; u_{pi}, k_{Fi}). \tag{176}$$

Plot of $\mathcal{E}_P(k_F a, N; u_{pi}, k_{Fi})$ for various values of $u_{pi}$ has been generated in FIG. 12. For $u_{pi} \ll 1$ the percentage deviations relative to the corresponding Lifshitz formula are about 20%. But, the Casimir energy itself is relatively small for $u_{pi} \ll 1$. Most remarkable deviation is in the modified expression for Casimir energy between two slabs having a non-zero limit as the thickness of one of the slabs goes to zero, $d \to 0$.

### A. Infinitesimally thin conducting plates

Using Eq. (167) which generalized the definition of plasma frequency as a guiding principle we claim that an infinitismally thin conducting slab will always be described by the model

$$(\varepsilon_i - 1)\zeta^2 = \frac{\lambda_i}{d_i}, \tag{177}$$

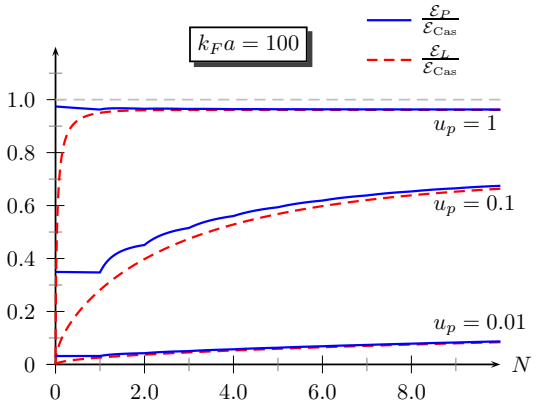


FIG. 12. Fractional Casimir energy including thickness dependence in dielectric function ($\mathcal{E}_P/\mathcal{E}_{\rm Cas}$) and fractional Lifshitz energy ($\mathcal{E}_L/\mathcal{E}_{\rm Cas}$) plotted with respect to thickness ($N = k_F d/\pi$) for $k_F a = 100$ for different values of plasma frequency ($u_p = \omega_p(\infty)/ck_F$).

where $\lambda_i$ is a parameter with dimensions of inverse length. ($\lambda_i \to \lambda_i c^2,\ c = 1.$) $\lambda_i$ is independent of $d$, but in general will have frequency dependence.

Restricting ourselves to frequencies and wavelength of the order

$$\zeta^2 \ll \frac{\lambda_i}{d_i}, \qquad k^2 \ll \frac{\lambda_i}{d_i}, \tag{178}$$

which are good approximations for a thin plate, we make the following leading-order replacements:

$$\varepsilon_i \sim \frac{\lambda_i}{d_i \zeta^2}\left[1 + \mathcal{O}\left(\zeta^2 \frac{d_i}{\lambda_i}\right)\right], \tag{179a}$$

$$\kappa_i \sim \sqrt{\frac{\lambda_i}{d_i}}\left[1 + \mathcal{O}\left(\zeta^2 \frac{d_i}{\lambda_i}, \kappa^2 \frac{d_i}{\lambda_i}\right)\right]. \tag{179b}$$

While using the above approximations to calculate the Casimir energy between two slabs of finite thickness translates to bounding the limits of integrations in Eq. (130) as

$$\mathcal{E}(a, d_i; \varepsilon_i - 1) \to \mathcal{E}_{TP}(a, d_i; \lambda_i) \sim \frac{1}{2}\int_{-\sqrt{\frac{\lambda_i}{d_i}}}^{\sqrt{\frac{\lambda_i}{d_i}}} \frac{d\zeta}{2\pi}\left[\int_{-\sqrt{\frac{\lambda_i}{d_i}}}^{\sqrt{\frac{\lambda_i}{d_i}}} \frac{dk}{2\pi}\right]^2 \Big\{\cdots\Big\}, \tag{180}$$

where 'TP' denotes thin plate, and the curly bracket represents the corresponding term in Eq. (130). Rescaling the integral parameters with $a$ then tells us that the thin plate approximation gives a good estimate of Casimir energy in the regime

$$\frac{d_i}{a} \ll \lambda_i a. \tag{181}$$

This has been illustrated in FIG. 13 where we plot the the ratio of Casimir energy with the cutoff limits over the complete integral limits. The approximation contributes to less than 10% error for $d < 10\,\lambda a^2$.

Using the leading-order replacements in Eq. (179) we can further derive

$$\alpha_i \sim 1, \qquad \bar{\alpha}_i \sim -1, \qquad \frac{1}{\Delta_i} \sim \frac{\lambda_i}{\lambda_i + 2\kappa}, \qquad \frac{1}{\bar{\Delta}_i} \sim \frac{\lambda_i}{\lambda_i + 2\frac{\zeta^2}{\kappa}}. \tag{182}$$

The above thin plate approximations when substituted in Eq. (130) leads to a non-zero contribution to Casimir energy given as

$$\mathcal{E}_{TP}(a, \lambda_i) = \frac{1}{2}\int_{-\infty}^{\infty}\frac{d\zeta}{2\pi}\int \frac{d^2k}{(2\pi)^2}\left\{\ln\left[1 - t_1(\kappa)t_2(\kappa)\,e^{-2\kappa a}\right] + \ln\left[1 - t_1\left(\tfrac{\zeta^2}{\kappa}\right)t_2\left(\tfrac{\zeta^2}{\kappa}\right)\,e^{-2\kappa a}\right]\right\}, \tag{183}$$

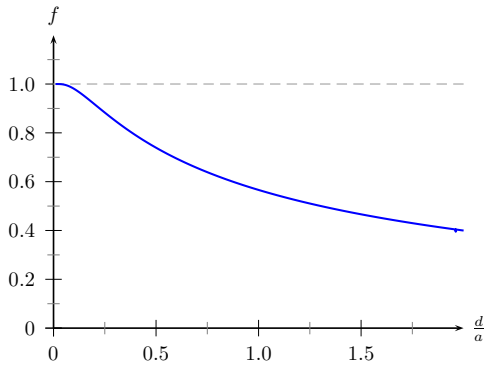


FIG. 13. Fractional error in Casimir energy due to thin plate approximation as a function of $d/a$ for $\lambda a = 1$.

where

$$t_i(\kappa) = \frac{\lambda_i}{\lambda_i + 2\kappa}. \tag{184}$$

We note the feature that the magnetic contribution to the Casimir energy in the thin plate limit is obtained by the replacement

$$\kappa \to \frac{\zeta^2}{\kappa} \tag{185}$$

inside the transition coefficients of the electric contribution. This is the modification of the replacement observed in Eq. (121) in the thin plate limit approximation. This is a generic feature of the thin plate approximation and was observed in the calulation of lateral Casimir force between corrugated thin plates too [22].

### 1. *Thin plate limit from the outset–A δ-function plate*

It is of interest to ask if infinitismally thin plates can be described using $\delta$-function potentials. To answer this assertively we begin by replacing the potentials in Eq. (102) with its $\delta$-function limits after introducing $d_i$'s in the expression. Thus, we consider

$$V_i(z) = \frac{\lambda_i}{\zeta^2}\,\delta(z - a_i), \qquad i = 1, 2. \tag{186}$$

Most of the discussion in Section IV remains the same with the change appearing in the following expressions:

$$\begin{aligned} K^E_{d_i\to 0}(i\zeta, k) &= \lambda_{p1}\lambda_{p1}\left[g^E_{1⑨}(z', z; i\zeta, k) g^E_{2④}(z, z'; i\zeta, k)\right]_{\substack{z=b_1\\ z'=a_2}} \\ &= \mu^E_{1,d_1\to 0}(i\zeta, k)\mu^E_{2,d_2\to 0}(i\zeta, k), \qquad (187) \\ \operatorname{tr}\mathbf{K}^H_{d_i\to 0}(i\zeta, k) &= \frac{\lambda_{p1}}{\varepsilon_1}\frac{\lambda_{p2}}{\varepsilon_2}\left[\left(1 - \frac{\kappa}{\zeta^2}\frac{\partial}{\partial z}\right)\left(1 + \frac{\kappa}{\zeta^2}\frac{\partial}{\partial z'}\right) g^H_{1⑨}(z', z) g^H_{2④}(z, z')\right]_{\substack{z=b_1\\ z'=a_2}} \\ &= \mu^H_{1,d_1\to 0}(i\zeta, k)\mu^H_{2,d_2\to 0}(i\zeta, k), \qquad (188) \\ & \qquad (189) \end{aligned}$$

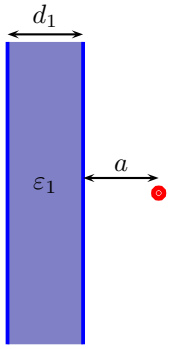


FIG. 14. Atom in front of a dielectric slab.

Using

$$\begin{aligned}\mu^E_{i,d_i\to 0}(i\zeta,k) &= \frac{\lambda_i}{\lambda_i+2\kappa}\frac{1}{2}u^E_{i,d_i\to 0}(a_i)\\ &= \frac{\lambda_i}{\lambda_i+2\kappa}\,e^{-\kappa a}, \qquad (190)\\ \mu^H_{i,d_i\to 0}(i\zeta,k) &= -\frac{\lambda_i}{\lambda_i+2\frac{\zeta^2}{\kappa}}\frac{1}{2}\sqrt{\frac{d_i}{\lambda_i}}\left[\frac{\partial}{\partial z}u^H_{i,d_i\to 0}(z)\right]_{z=a_i}\\ &= -\frac{\lambda_i}{\lambda_i+2\frac{\zeta^2}{\kappa}}\,e^{-\kappa a}, \qquad (191)\end{aligned}$$

which leads to the same result as obtained in Eq. (183).

Taking $\lambda_i \to \infty$ limit leads to the standard Casimir energy between two perfectly conducting plates. This agrees with the results given in [23] for the Casimir energy for the two perfectly conducting thin plates.

## VII. CASIMIR-POLDER ENERGY FOR THICK AND THIN CONDUCTORS

In [23] Bordag found that the Casimir-Polder force for the infinitesimally thin perfect conductor is 13% less than the standard value while for a thick conductor it is unchanged. It is therefore relevant to check these results using our method for taking the thin plate limit. In this Section we present the Casimir-Polder energy for an atom in front of a thick dielectric slab and thin conducting plate. We take the perfect conductor limit in both cases to obtain the standard Casimir-Polder result.

### A. Atom in front of a thick dielectric slab

Let us consider the physical situation of an atom in front of a dielectric slab shown in Figure 14. The background potential for this system is described by

$$\begin{aligned}V(\mathbf{x};i\zeta) &= V_1(\mathbf{x};i\zeta)+V_2(\mathbf{x};i\zeta)\\ &= (\varepsilon_1(i\zeta)-1)\left[\theta(z-a_1)-\theta(z-b_1)\right]+4\pi\boldsymbol{\alpha}_P(i\zeta)\delta^{(3)}(\mathbf{x}-\mathbf{x}_0). \qquad (192)\end{aligned}$$

where $\boldsymbol{\alpha}_P(i\zeta)$ is the polarizability tensor of the atom, which is located at $\mathbf{x}_0=(0,0,a_2)$. We have kept the frequency dependence of the permittivity to keep expressions general. Since the atom interacts weakly with the slab, only the single scattering term from the expansion of the multiple scattering formula given by Eq. (47) is important. Thus the

interaction energy is given by

$$\begin{aligned} E_{12}^{CP} &= -\frac{1}{2}\int_{-\infty}^{\infty}\frac{d\zeta}{2\pi}\,\mathrm{Tr}\,\mathbf{\Gamma}_1\cdot\mathbf{V}_1\cdot\mathbf{\Gamma}_0\cdot\mathbf{V}_2 \\ &= -\frac{1}{2}\int_{-\infty}^{\infty}\frac{d\zeta}{2\pi}\,[4\pi\boldsymbol{\alpha}_P(i\zeta)]\cdot\int d^3x\,\mathbf{\Gamma}_1(\mathbf{x}_0,\mathbf{x})\cdot\mathbf{V}_1(\mathbf{x})\cdot\mathbf{\Gamma}_0(\mathbf{x},\mathbf{x}_0) \\ &= -\frac{1}{2}\int_{-\infty}^{\infty}\frac{d\zeta}{2\pi}\,[4\pi\boldsymbol{\alpha}_P(i\zeta)]\cdot[\mathbf{\Gamma}_1-\mathbf{\Gamma}_0]\,. \end{aligned} \tag{193}$$

For an isotropic polarizable atom we have

$$E_{12}^{CP}(a,d_1,\varepsilon_1-1;\alpha_P)=\frac{1}{2}\int_{-\infty}^{\infty}\frac{d\zeta}{2\pi}\int_{-\infty}^{\infty}\frac{d^2k}{2\pi}\,[4\pi\alpha_P(i\zeta)]\,(\varepsilon_1(i\zeta)-1)K(k,\zeta;a,d_1), \tag{194}$$

where

$$K(k,\zeta;a,d_1)=\int_{a_1}^{b_1}dz\,\mathrm{tr}\,\boldsymbol{\gamma}_1(a_2,z;k,\zeta)\cdot\boldsymbol{\gamma}_0(z,a_2;k,\zeta). \tag{195}$$

Using Eqs. (55),(79), and (80) we can write the explicit form for the reduced free Green's dyadic as

$$\boldsymbol{\gamma}_0(z,z';i\zeta,k)=\begin{bmatrix} -\kappa^2 & 0 & -ik\kappa\,\eta(z-z') \\ 0 & \zeta^2 & 0 \\ -ik\kappa\,\eta(z-z') & 0 & k^2 \end{bmatrix}\frac{1}{2\kappa}\,e^{-\kappa|z-z'|}, \tag{196}$$

where $\eta(z)=1$ if $z>0$, and $\eta(z)=-1$ if $z<0$. Using this and Eq. (75) we have the result

$$E_{12}^{CP}(a,d_1,\varepsilon_1-1;\alpha_P)=-\frac{1}{2}\int_{-\infty}^{\infty}\frac{d\zeta}{2\pi}[4\pi\alpha_P(i\zeta)]\int\frac{d^2k}{(2\pi)^2}\,e^{-2\kappa a}\left[\frac{(\kappa^2-k^2)}{2\kappa}\frac{\alpha_1}{\Delta_1}-\frac{(\kappa^2+k^2)}{2\kappa}\frac{\bar{\alpha}_1}{\bar{\Delta}_1}\right], \tag{197}$$

which is the expected result found in the literature [16]. In the thick-plate limit ($d\to\infty$) we have

$$E_{12}^{CP}(a,\infty,\varepsilon_1-1;\alpha_P)=-\frac{1}{2}\int_{-\infty}^{\infty}\frac{d\zeta}{2\pi}[4\pi\alpha_P(i\zeta)]\int\frac{d^2k}{(2\pi)^2}\,e^{-2\kappa a}\left[\frac{(\kappa^2-k^2)}{2\kappa}\alpha_1-\frac{(\kappa^2+k^2)}{2\kappa}\bar{\alpha}_1\right]. \tag{198}$$

If the polarizability is independent of the frequency then taking the perfect conductor limit ($\varepsilon_1\to\infty$) we reproduce the standard Casimir-Polder energy

$$E_{12}^{CP}(a,d_1,\infty;\alpha_P)=-\frac{3\alpha_P}{8\pi a^4}. \tag{199}$$

### B. Atom in front of a infinitesimally thin conducting plate

We can take the thin-plate limit ($d\to 0$) in Eq. (197) described in Sections V and VI A

$$E_{12}^{CP}(a,\lambda_1;\alpha_P)=-\frac{1}{2}\int_{-\infty}^{\infty}\frac{d\zeta}{2\pi}[4\pi\alpha_P(i\zeta)]\int_{-\infty}^{\infty}\frac{d^2k}{(2\pi)^2}\,e^{-2\kappa a}\Big[\frac{(\kappa^2-k^2)}{2\kappa}\frac{\lambda_1}{\lambda_1+2\kappa}+\frac{(\kappa^2+k^2)}{2\kappa}\frac{\lambda_1}{\lambda_1+2\frac{\zeta^2}{\kappa}}\Big]. \tag{200}$$

In the perfect conductor limit $\lambda_1\to\infty$

$$E_{12}^{CP}(a,\infty;\alpha_P)=-\frac{1}{2}\int_{-\infty}^{\infty}\frac{d\zeta}{2\pi}[4\pi\alpha_P(i\zeta)]\int_{-\infty}^{\infty}\frac{d^2k}{(2\pi)^2}\,e^{-2\kappa a}\kappa, \tag{201}$$

which when $\alpha_P(i\zeta)$ is independent of frequency gives the standard Casimir Polder result

$$E_{12}^{CP}(a,\infty;\alpha_P)=-\frac{3\alpha_P}{8\pi a^4}. \tag{202}$$

Thus a $\delta$-function perfectly conducting thin-plate interacting with an atom reproduces the Casimir-Polder energy exactly, which we believe is the correct result. For a perfect conductor the field goes to zero at the surface and the skin depth of the material is zero as well. Therefore the region beyond the slab or plate does not contribute to the energy. We believe that the thickness of the material should not affect the perfect conductor results.

### C. Discussion

As we see in previous subsection our result does not agree with Bordag's claim of reduction of 13% in the Casimir Polder energy for an atom in front of a thin conductor [23]. He attributes the origin of this discrepancy to the freedom in choice of the boundary condition for the normal component of the electric field $E_\perp$. For a perfect conductor the required boundary conditions are $E_\parallel = H_\perp = 0$. This, according to him leaves room to impose different boundary conditions on the normal component of the electric field in different cases. However, notice that if the boundary conditions for perfect conductor are used in conjunction with the Maxwell's equation ($\boldsymbol{\nabla} \cdot \mathbf{E} = 0$) for a charge–and current-less space then the condition on the third component is unambiguously fixed. This according to him is the case for the thick material, while for the thin material the third component remains free. He shows the calculation for the energy, for the two cases, by calculating propagator for the photon field. We can easily check that the electric field obtained from both the forms are same, which indicates that the energy obtained from the two forms should also be the same. This seems to be a puzzling result, which we intend to discuss with him personally.

In this context we should also point out previous work by Fetter in [24], where he considers the motion of an electron in the vicinity of a thin-plate modeled by the electron gas in presence of neutralizing background and shows that the dynamics of the electron is different in this case from the bulk material. He, however, considers only real conductors and is not considering quantum vacuum effects.

## VIII. GRAPHENE

Graphene is a single layer of graphite. The carbon atoms in graphene arrange to form a two-dimensional hexagonal lattice with each side of a hexagon measuring 0.142 nm. The interlayer separation between the layers in graphite is 0.337 nm. It is of interest to calculate the Casimir interaction energy per unit area, $\mathcal{E}_{\text{g-g}}$, between two graphene sheets. This is expected to be related to the interlayer binding energy of graphite. If we sum over all the two-body contributions to the the interlayer binding energy of graphite, and ignore all other many-body contributions, we obtain the estimate for the binding energy of graphite as the series

$$\mathcal{E}^{\text{BE}}_{\text{graphite}} = 2\mathcal{E}_{\text{g-g}} \left[ \frac{1}{1^3} + \frac{1}{2^3} + \frac{1}{3^3} + \dots \right] = 2\zeta(3)\mathcal{E}_{\text{g-g}}. \tag{203}$$

In arriving at the above expression we have used the fact that

$$\mathcal{E}_{\text{g-g}} = g_{\text{g-g}}(\pi\alpha)\mathcal{E}_{\text{Cas}}, \tag{204}$$

where $\mathcal{E}_{\text{Cas}}$ is the Casimir energy between parallel perfectly conducting plates given by Eq. (135a), and $g(\alpha)$ is a constant completely given in terms of the fine structure constant $\alpha$. Factor of $n^3$ results from the $a^3$ dependence. Exfoliation energy of graphite is the energy required to strip graphene from a semi-infinite graphite. This is estimated by ignoring the factor of 2 in Eq. (203) which yields

$$\mathcal{E}^{\text{EE}}_{\text{graphite}} = \zeta(3)\mathcal{E}_{\text{g-g}}. \tag{205}$$

There is considerable amount of experimental data for the binding energy and exfoliation energy of graphite, though with high error bars. In this work we shall content ourselves with predicting the values in the right ballpark.

### A. Dielectric function for graphene

Our primary goal will be to evaluate the Casimir interaction energy between two graphene sheets. We begin with Eq. (183) with the refelection coefficients given using Eq. (177) which we rewrite in the form

$$\lambda_g = (\varepsilon_g - 1)\zeta^2 d, \tag{206}$$

where $d$ is the thickness of a graphene sheet and $\varepsilon_g$ is the dielectric permittivity of the graphene sheet. Thus, our problem reduces to determining the dielectric model for graphene. To this end we note that conduction electrons in undoped graphene (a 2-dimensional structure) in the lowest Brillouin zone are decribed by a Diriac-like dispersion relation [25]

$$E = v_F|\mathbf{p}|, \tag{207}$$

where $\mathbf{p}$ is the momentum of the electrons in the plane of graphene, and $v_F = c/300$ is determined in terms of the lattice parameters. Introducing a mass which is loosely equivalent to considering doped graphene we have

$$E^2 = \frac{v_F^2}{c^2} p^2 c^2 + m^2 c^4, \tag{208}$$

which leads to the Dirac's dispersion relation for $v_F = c$. We introduced $c$ in the expression for clarity. In terms of Diriac-like matrices we can write

$$E = \tilde{\gamma}_0 \tilde{\boldsymbol{\gamma}} \cdot \mathbf{p} + m\tilde{\gamma}_0, \tag{209}$$

where the modified $\gamma$-matrices are defined as $\tilde{\gamma}^\mu = (\gamma, v_F \boldsymbol{\gamma})$ and satisfy the anti-commutation relations

$$\{\tilde{\gamma}^\mu, \tilde{\gamma}^\nu\} = -2\eta^\mu{}_\lambda \eta^\nu{}_\sigma g^{\lambda\sigma}, \qquad \{\gamma^\mu, \gamma^\nu\} = -2g^{\mu\nu}, \qquad \eta^\mu{}_\nu = \mathrm{diag}(1, \mathbf{v}_F), \qquad \mu = 0, 1, 2, \ldots, D, \tag{210}$$

with $D$ being the number space dimensions in a $(D+1)$-dimensional space-time. The conduction electrons in graphene are confined to be in a 2-dimensional sheet in (3+1)-dimensional space-time, thus $D = 2$. The interaction between conduction electrons and electromagnetic fields will be described by the action

$$W = i \int d^2x \int dt \left[ -\frac{1}{4} \int dz\, F_{\mu\nu} F^{\mu\nu} - \int_0^d dz\, \psi^\dagger \tilde{\gamma}^0 \left\{ \tilde{\gamma}^\mu \left( \frac{1}{i} \partial_\mu - eA_\mu \right) + m \right\} \psi \right], \tag{211}$$

in which the electrons are confined to move in the graphene sheet. We shall assume that the Dirac fields have no knowledge of the thickness $d$. This probably needs to be taken care of more rigorously if one intends to compare our final results more precisely with experiments. But, as we mentioned earlier our goal will be simply to get the numbers in the right ballpark.

The dielectric permittivity in this model is given by

$$[\varepsilon^{ij}(\mathbf{k}, \omega) - \delta^{ij}]\omega^2 = \Pi^{ij}(\mathbf{k}, \omega; m), \tag{212}$$

where the right hand side is given in terms of the vacuum polarization contribution

$$i\Pi^{\mu\nu}(\mathbf{k}, \omega; m) = -\frac{e^2}{d} \mathrm{tr} \int \frac{d^{D+1}p}{(2\pi)^{D+1}}\, \tilde{\gamma}^\mu \frac{1}{[m + \tilde{\gamma} p]} \tilde{\gamma}^\nu \frac{1}{[m + \tilde{\gamma}(p - k)]}. \tag{213}$$

In terms of redefined momentums, $\tilde{p}^\mu = \eta^\mu{}_\nu p^\nu$, after evaluating the traces over the gamma indices we have

$$i\Pi^{\mu\nu}(\mathbf{k}, \omega; m) = -\frac{e^2}{d} \frac{1}{v_F^D} \int \frac{d^{D+1}\tilde{p}}{(2\pi)^{D+1}}\, \frac{1}{[m^2 + \tilde{p}^2]} \frac{1}{[m^2 + (\tilde{p} - \tilde{k})^2]} T^{\mu\nu}, \tag{214}$$

where

$$T^{\mu\nu} = -4[m^2 + \tilde{p}(\tilde{p} - \tilde{k})]\eta^\mu{}_\lambda \eta^\nu{}_\sigma g^{\lambda\sigma} + 4[\tilde{p}^\sigma (\tilde{p} - \tilde{k})^\lambda + \tilde{p}^\lambda (\tilde{p} - \tilde{k})^\sigma] \eta^\mu{}_\lambda \eta^\nu{}_\sigma. \tag{215}$$

Using the integral representation

$$\frac{1}{M - i\delta} = i \int_0^\infty ds\, e^{-is(M - i\delta)} \tag{216}$$

to invert the denominators and then using the substitutions $s_1 = su$, $s_2 = s(1 - u)$, we can write

$$i\Pi^{\mu\nu}(\mathbf{k}, \omega; m) = -\frac{e^2}{d} \frac{1}{v_F^D} \int_0^\infty s ds\, e^{-ism^2} \int_0^1 du\, e^{-is\tilde{k}^2 u(1-u)} \int \frac{d^{D+1}\tilde{p}}{(2\pi)^{D+1}} (T_1^{\mu\nu} + T_2^{\mu\nu} + T_3^{\mu\nu}) e^{-is(\tilde{p} - u\tilde{k})^2}, \tag{217}$$

where

$$T_1^{\mu\nu} = 4u(1 - u) \left[ \tilde{k}^2 g^{\lambda\sigma} - 2\tilde{k}^\lambda \tilde{k}^\sigma \right] \eta^\mu{}_\lambda \eta^\nu{}_\sigma, \tag{218}$$

$$T_2^{\mu\nu} = -4 \left[ \{m^2 + (\tilde{p} - u\tilde{k})^2\} g^{\lambda\sigma} - 2(\tilde{p} - u\tilde{k})^\lambda (\tilde{p} - u\tilde{k})^\sigma \right] \eta^\mu{}_\lambda \eta^\nu{}_\sigma, \tag{219}$$

$$T_3^{\mu\nu} = -4(2u - 1) \left[ \tilde{k} \cdot (\tilde{p} - u\tilde{k}) g^{\lambda\sigma} - \{\tilde{k}^\lambda (\tilde{p} - u\tilde{k})^\sigma + \tilde{k}^\sigma (\tilde{p} - u\tilde{k})^\lambda\} \right] \eta^\mu{}_\lambda \eta^\nu{}_\sigma. \tag{220}$$

After the Euclidean rotation, $\tilde{p}^0 \to i\tilde{p}^0$, we can evaluate

$$\int \frac{d^{D+1}\tilde{p}}{(2\pi)^{D+1}}\, e^{-is(\tilde{p}-u\tilde{k})^2} = \frac{i^{(1-D)/2}}{(4\pi s)^{(1+D)/2}}, \tag{221}$$

$$\int \frac{d^{D+1}\tilde{p}}{(2\pi)^{D+1}}\, e^{-is(\tilde{p}-u\tilde{k})^2}(\tilde{p}-u\tilde{k})^\mu = 0, \tag{222}$$

$$\int \frac{d^{D+1}\tilde{p}}{(2\pi)^{D+1}}\, (\tilde{p}-u\tilde{k})^2 e^{-is(\tilde{p}-u\tilde{k})^2} = \frac{(1+D)}{2}\frac{1}{is}\frac{i^{(1-D)/2}}{(4\pi s)^{(1+D)/2}}, \tag{223}$$

$$\int \frac{d^{D+1}\tilde{p}}{(2\pi)^{D+1}}\, (\tilde{p}-u\tilde{k})^\lambda(\tilde{p}-u\tilde{k})^\sigma e^{-is(\tilde{p}-u\tilde{k})^2} = \frac{g^{\lambda\sigma}}{2is}\frac{i^{(1-D)/2}}{(4\pi s)^{(1+D)/2}}, \tag{224}$$

which immediately impies that $T_3^{\mu\nu}$ does not contribute. Rest of the two contributions lets us write

$$\Pi^{\mu\nu}(\mathbf{k},\omega;m) = \Pi_1^{\mu\nu}(\mathbf{k},\omega;m) + \Pi_2^{\mu\nu}(\mathbf{k},\omega;m), \tag{225}$$

where

$$\Pi_1^{\mu\nu}(\mathbf{k},\omega;m) = \frac{1}{2}\frac{1}{v_F^D}\left[2\tilde{k}^\lambda\tilde{k}^\sigma - \tilde{k}^2 g^{\lambda\sigma}\right]\eta^\mu{}_\lambda\eta^\nu{}_\sigma\,\Pi_D(\mathbf{k},\omega;m), \tag{226}$$

where

$$\Pi_D(\mathbf{k},\omega;m) = -\frac{1}{d}\frac{8e^2}{(4\pi i)^{(1+D)/2}}\int_0^\infty \frac{ds}{s}s^{(3-D)/2}e^{-ism^2}\int_0^1 du\, u(1-u)\, e^{-is\tilde{k}^2u(1-u)}. \tag{227}$$

Evaluation of $\Pi_2^{\mu\nu}(\mathbf{k},\omega;m)$ involves the integral

$$\int \frac{d^{D+1}p}{(2\pi)^{D+1}}\, T_2^{\mu\nu}e^{-is(\tilde{p}-u\tilde{k})^2} = -4\eta^\mu{}_\lambda\eta^\nu{}_\sigma g^{\lambda\sigma}\frac{1}{(4\pi is)^{(1+D)/2}}\left[im^2 + \frac{(D-1)}{2s}\right], \tag{228}$$

and integrating by parts using

$$\frac{d}{ds}\left[\frac{1}{s^{(D-1)/2}}\, e^{-ism^2}\right] = -\frac{1}{s^{(D-1)/2}}\left[im^2 + \frac{(D-1)}{2s}\right]e^{-ism^2}, \tag{229}$$

and throwing away the surface term we have

$$\Pi_2^{\mu\nu}(\mathbf{k},\omega;m) = \frac{1}{2}\frac{1}{v_F^D}\tilde{k}^2\eta^\mu{}_\lambda\eta^\nu{}_\sigma g^{\lambda\sigma}\,\Pi_D(\mathbf{k},\omega;m). \tag{230}$$

Using Eqs. (226) and (230) in Eq. (225) we have

$$\Pi^{\mu\nu}(\mathbf{k},\omega;m) = \frac{1}{v_F^D}\left[\tilde{k}^\lambda\tilde{k}^\sigma - \tilde{k}^2 g^{\lambda\sigma}\right]\eta^\mu{}_\lambda\eta^\nu{}_\sigma\,\Pi_D(\mathbf{k},\omega;m). \tag{231}$$

Substituting $u = (1+v)/2$ in Eq. (227) ans performing the $s$-integral after Euclidean rotation ($s \to -is$) lets us write

$$\Pi_D(\mathbf{k},\omega;m) = \frac{2e^2\Gamma\left(\frac{3-D}{2}\right)}{(4\pi)^{(1+D)/2}}\frac{1}{d}\int_0^1 dv \frac{(1-v^2)}{\left[m^2 + \frac{1}{4}\tilde{k}^2(1-v^2)\right]^{(3-D)/2}}. \tag{232}$$

We can evaluate the limiting cases

$$\Pi_D(\mathbf{k},\omega;0) = \frac{1}{d}\frac{e^2\Gamma\left(\frac{3-D}{2}\right)\Gamma\left(\frac{1+D}{2}\right)}{\pi^{D/2}2^{(1+D)}\Gamma\left(1+\frac{D}{2}\right)}\left(\frac{2}{\tilde{k}}\right)^{3-D}, \qquad -1 < D < 3, \tag{233}$$

$$\Pi_D(0,0;m) = \frac{1}{d}\frac{4e^2\Gamma\left(\frac{3-D}{2}\right)}{3(4\pi)^{(1+D)/2}}\frac{1}{m^{3-D}}, \qquad D < 3. \tag{234}$$

For $D = 2$ which is the case of our interest we have

$$\Pi_2(\mathbf{k}, \omega; 0) = \frac{e^2}{8} \frac{1}{\tilde{k} d}, \tag{235}$$

$$\Pi_2(0, 0; m) = \frac{e^2}{6\pi} \frac{1}{md}. \tag{236}$$

We note that in $D = 2$ the contribution from vacuum polarization at zero momentum vanishes in the limit $d \to \infty$ for non-zero mass. Thus, there is no (re)normalization necessary.

At this stage it is worth pointing out that a more satisfatory exercise would be to compute the above for a sheet of finite thickness and then take the limit $d \to 0$, which we shall complete elesewhere. We do not expect the qualitative behaviour of the results to change.

For an isotropic medium, taking the trace in Eq. (212) we have

$$\varepsilon(\mathbf{k}, \omega) - 1 = -\left(1 - \frac{v_F^2}{2} \frac{\mathbf{k}^2}{\omega^2}\right) \Pi_2(\mathbf{k}, \omega; 0). \tag{237}$$

Setting $\mathbf{k} = 0$ ($\tilde{k} \to i\omega$) we have

$$\varepsilon(0, \omega) - 1 = -\Pi_2(0, \omega; 0) = -\frac{\sigma}{i\omega}, \tag{238}$$

where we identified the conductivity

$$\sigma = \frac{e^2}{8d}. \tag{239}$$

For graphene we have 2 electron states (4 two-component spinor states) in the lowest Brillouin zone [25], thus

$$\sigma_g = 2\frac{e^2}{8d} = \frac{\pi\alpha}{d}. \tag{240}$$

Using Eq. (240) in Eq. (206) we have for graphene

$$\lambda_g = \pi\alpha\zeta. \tag{241}$$

### B. Casimir interaction energy between two graphene sheets

Using Eq. (241) in Eq. (183) we have

$$\mathcal{E}_{\text{g-g}} = \frac{1}{2} \int_{-\infty}^{\infty} \frac{d\zeta}{2\pi} \int \frac{d^2k}{(2\pi)^2} \left\{ \ln\left[1 - \left(\frac{\pi\alpha\zeta}{\pi\alpha\zeta + 2\kappa}\right)^2 e^{-2\kappa a}\right] + \ln\left[1 - \left(\frac{\pi\alpha\zeta}{\pi\alpha\zeta + 2\kappa\frac{\zeta^2}{\kappa^2}}\right)^2 e^{-2\kappa a}\right]\right\}, \tag{242}$$

which lets us read out $g_{\text{g-g}}(\alpha)$ in Eq. (204) to be

$$g_{\text{g-g}}(\pi\alpha) = -\frac{720}{\pi^2} \frac{1}{2} \int_{-\infty}^{\infty} \frac{d\zeta}{2\pi} \int \frac{d^2k}{(2\pi)^2} \left\{ \ln\left[1 - \left(\frac{\pi\alpha\zeta}{\pi\alpha\zeta + 2\kappa}\right)^2 e^{-2\kappa}\right] + \ln\left[1 - \left(\frac{\pi\alpha\zeta}{\pi\alpha\zeta + 2\kappa\frac{\zeta^2}{\kappa^2}}\right)^2 e^{-2\kappa}\right]\right\}. \tag{243}$$

After scaling the integral variables with $a$ and introducing spherical polar coordinates we can write

$$g_{\text{g-g}}(\pi\alpha) = -\frac{45}{2\pi^4} \int_0^{\infty} s^2 ds \int_0^1 dt \left\{ \ln\left[1 - \left(\frac{\pi\alpha}{\pi\alpha + \frac{2}{|t|}}\right)^2 e^{-s}\right] + \ln\left[1 - \left(\frac{\pi\alpha}{\pi\alpha + 2|t|}\right)^2 e^{-s}\right]\right\}. \tag{244}$$

The fine structure constant is $\alpha = 1/137$. Using Eq. (243) we numerically evaluate $g_{\text{g-g}}(\pi\alpha) = 0.005$. Thus, using Eq. (204) we have

$$\mathcal{E}_{\text{g-g}} = 0.005\, \mathcal{E}_{\text{Cas}}. \tag{245}$$

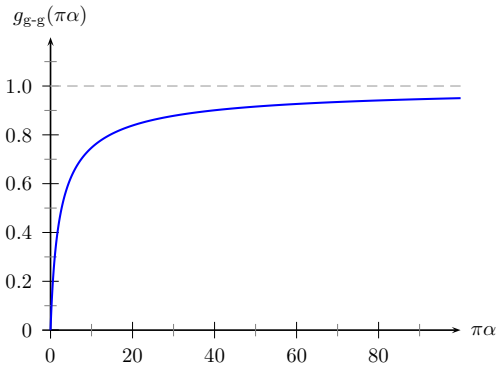


FIG. 15. Ineteraction energy between two graphene sheets scaled with Casimir energy for conducting plates plotted with $\pi\alpha$.

The above expression satisfies $g_{\text{g-g}}(\infty) = 1$, which implies that the perfect conductor limit is got in the limit $\alpha \to \infty$. This is also seen in the plot of $g_{\text{g-g}}(\pi\alpha)$ versus $\pi\alpha$ in Fig. 15. It is of interest to see how weak limits of these expressions compare with the exact results. We expand Eqs. (244) in $\alpha$ to yield

$$g_{\text{g-g}}(\pi\alpha) = \frac{45}{2\pi^4}\,\pi\alpha + \mathcal{O}(\pi\alpha)^2 = 0.005 + \mathcal{O}(\pi\alpha)^2. \tag{246}$$

The weak approximation reproduces the graphene-graphene interaction energy accurately. This suggests the far-reaching conclusion that weak approximations can be successfully employed to predict Casimir interactions between fullerene molecules (which are graphene sheets folded to form closed structures by replacing few of the hexagonal rings with pentagons). A very general expression for Casimir-Polder (van der Waals-London) forces of arbitrary shapes was derived in [26]. A deduction along these lines suggests the following expression for the interaction energy between fullerene molecules

$$E_{\text{f-f}} = -\frac{3\alpha}{32\pi^2}\int_{s_1} d^2r_{1\perp}\int_{s_2} d^2r_{2\perp}\frac{1}{|\mathbf{r}_1 - \mathbf{r}_2|^5}, \tag{247}$$

where the shapes of the surfaces of the fullerene molecules are given by surfaces $s_1$ and $s_2$. We shall derive the above expression more authoritatively elesewhere.

### C. Interlayer binding energy of graphite

For $a = 0.337\,\text{nm}$ we have

$$\mathcal{E}_{\text{Cas}} = \frac{\pi^2}{720\,(0.337\,\text{nm})^3} = 11.289\,\text{J/m}^2 = 1.4027\,\text{eV/atom}. \tag{248}$$

Thus, using Eqs. (203) and (205) we have

$$\mathcal{E}^{\text{BE}}_{\text{graphite}} = 0.013\,\mathcal{E}_{\text{Cas}}, \qquad \mathcal{E}^{\text{EE}}_{\text{graphite}} = 0.007\,\mathcal{E}_{\text{Cas}}, \tag{249}$$

which are on the lower side of experimental measurements.

In Section VI A we investigated the parameter regime in which the thin plate approximations are good. Using Eqs. (240) and (241) we obtain the restriction $\zeta \ll \sigma_g$ which implies

$$\frac{d}{a} \ll 2\pi\alpha \sim 0.05. \tag{250}$$

Validity check in the case of graphene calls for the definition of thickness $d$ of a graphene sheet. But, it is clear that the condition is not strictly met for separation distances in graphite. Thus, our results on graphite should be taken with a grain of salt. Nevertheless, thin plate approximation seems very much in experimental reach.

### D. Casimir interaction energy between graphene and an ideal metal

An ideal metal involves replacing $t_i(\kappa) \to 1$ in Eq. (183). This leads to

$$\mathcal{E}_{\text{g-metal}} = g_{\text{g-m}}(\pi\alpha)\mathcal{E}_{\text{Cas}}, \tag{251}$$

with

$$g_{\text{g-m}}(\pi\alpha) = -\frac{45}{2\pi^4}\int_0^\infty s^2 ds \int_0^1 dt \Bigg\{ \ln\left[1 - \left(\frac{\pi\alpha}{\pi\alpha + \frac{2}{t}}\right) e^{-s}\right] + \ln\left[1 - \left(\frac{\pi\alpha}{\pi\alpha + 2t}\right) e^{-s}\right]\Bigg\}, \tag{252}$$

which is different from the case of graphene-graphene interaction by a power in the reflection coefficients. The $s$-integral can be evaluated to yield

$$g_{\text{g-m}}(\pi\alpha) = \frac{45}{\pi^4}\int_0^1 dt \left[\text{Li}_4\left(\frac{\pi\alpha}{\pi\alpha + \frac{2}{t}}\right) + \text{Li}_4\left(\frac{\pi\alpha}{\pi\alpha + 2t}\right)\right], \tag{253}$$

where $\text{Li}_4(z)$ is the polylogarithm function. The above numerically evaluates to 0.027. Thus,

$$\mathcal{E}_{\text{g-metal}} = 0.027\,\mathcal{E}_{\text{Cas}}. \tag{254}$$

It is again of interest to see how weak limit of this expression compares with the exact result. We expand Eq.(252) in $\alpha$ to yield

$$g_{\text{g-m}}(\pi\alpha) = \frac{45}{4\pi^4}\pi\alpha\left[1 + 2\ln\left(1 + \frac{2}{\pi\alpha}\right)\right] + \mathcal{O}(\pi\alpha)^2 = 0.026 + \mathcal{O}(\pi\alpha)^2. \tag{255}$$

Thus, weak approximation is again pretty accurate in estimating the graphene-metal situation.

## ACKNOWLEDGMENTS

We thank Aram Saharian for very helpful suggestions and comments during the calculation on graphene.

[1] L. Brillouin, *Wave propagation and group velocity* (Academic Press Inc., London, 1960).
[2] R. de L. Kronig, "On the theory of dispersion of X-rays," J. Opt. Soc. Am. **12**, 547–557 (Jun 1926).
[3] Julian. Schwinger, Jr. DeRaad, Lester L., Kimball A. Milton, and Wu-yang Tsai, *Classical electrodynamics*, Advanced book program (1998).
[4] J. Schwinger, "The algebra of microscopic measurement," Proc. Nat. Acad. Sci. **45**, 1542 (1959).
[5] J. Schwinger, "The geometry of quantum states," Proc. Nat. Acad. Sci. **46**, 257 (1960).
[6] J. Schwinger, "Unitary operator bases," Proc. Nat. Acad. Sci. **46**, 570 (1960).
[7] J. Schwinger, "Unitary transformations and the action principle," Proc. Nat. Acad. Sci. **46**, 883 (1960).
[8] J. Schwinger, "The special canonical group," Proc. Nat. Acad. Sci. **46**, 1401 (1960).
[9] J. Schwinger, "Quantum variables and the action principle," Proc. Nat. Acad. Sci. **47**, 1075 (1961).
[10] J. Schwinger, "Exterior algebra and the action principle, I," Proc. Nat. Acad. Sci. **48**, 603 (1962).
[11] J. Schwinger, *Particles, sources, and fields. Volume 1* (Reading, Mass., USA, (1970) 425 p).
[12] Kimball A. Milton, Lester L. DeRaad, Jr., and Julian S. Schwinger, "Casimir selfstress on a perfectly conducting spherical shell," Ann. Phys. **115**, 388 (1978).
[13] Kimball A. Milton and Jef Wagner, "Multiple scattering methods in Casimir calculations," J. Phys. **A41**, 155402 (2008), arXiv:0712.3811 [hep-th].
[14] P. M. Morse and H. Feshbach, *Methods of theoretical Physics* (McGraw-Hill book companya, NY, USA, 1953).
[15] Julian S. Schwinger, Jr. DeRaad, Lester L., and Kimball A. Milton, "Casimir effect in dielectrics," Annals Phys. **115**, 1–23 (1978).
[16] K. A. Milton, *The Casimir effect: Physical manifestations of zero-point energy* (World Scientific, River Edge, USA, 2001).
[17] Kimball A. Milton, Jef Wagner, Prachi Parashar, and Iver Brevik, "Casimir energy, dispersion, and the Lifshitz formula," Phys. Rev. D **81**, 065007 (Mar 2010).
[18] E. M. Lifshitz, Zh. Eksp. Teor. Fiz. **29**, 94 (1956), [English transl.: *Soviet Phys. JETP* 2:73, 1956].
[19] Bo E. Sernelius, *Surface modes in physics* (WILEY-VCH, Verlag Berlin GmbH, Berlin (Bundesrepublik Deutschland), 2001).

[20] Landau, Z. Phys. **64**, 629 (1930).
[21] Neil W. Ashcroft and N. David Mermin, *Solid state physics* (Holt, Rinehart and Winston, USA, 1976).
[22] Prachi Parashar, Kimball A. Milton, Ines Cavero-Pelaez, and K. V. Shajesh, "Electromagnetic Non-contact Gears: Prelude," (2010), arXiv:1001.4105 [cond-mat.other].
[23] Michael Bordag, "Reconsidering the quantization of electrodynamics with boundary conditions and some measurable consequences," Phys. Rev. **D70**, 085010 (2004), arXiv:hep-th/0403222.
[24] Alexander L. Fetter, "Electrodynamics of a layered electron gas. I. Single layer," Annals of Physics **81**, 367 – 393 (1973).
[25] P. R. Wallace, "The band theory of graphite," Phys. Rev. **71**, 622–634 (May 1947).
[26] Kimball A. Milton, Prachi Parashar, and Jef Wagner, "Exact Results for Casimir Interactions between Dielectric Bodies: The Weak-Coupling or van der Waals Limit," Phys. Rev. Lett. **101**, 160402 (Oct 2008).